T.C.

ALTINBAS UNIVERSITY

Institute of Graduate Studies

Mechanical Engineering

Numerical study of heat transfer aspects in cutting tools made of Al_2O_3, ZrB_2, TiB_2 and TiN

Master of Science

Supervisor

Asst. Prof. Dr. Suleyman BASTURK

Istanbul, 2020

Numerical study of heat transfer aspects in cutting tools made of Al_2O_3, ZrB_2, TiB_2 and TiN

by

Kamal F. Mohammed

Mechanical Engineering

Submitted to the Institute of Graduate Studies

in partial fulfillment of the requirements for the degree of

Master of Science

ALTINBAŞ UNIVERSITY

2020

The thesis titled "Numerical study of heat transfer aspects in cutting tools made of Al_2O_3, ZrB_2, TiB_2 and TiN" prepared and presented by Kamal F. Mohammed was accepted as a Master of Science Thesis in Mechanical Engineering.

_____	_____
Co-Supervisor	Asst. Prof. Dr. Suleyman BASTURK Supervisor

Thesis Defense Jury Members:

Prof. Dr. Osman Ergüven VATANDAŞ	Faculty of Engineering and Architecture, Istanbul Gelişim University	_____
Asst. Prof. Dr. Süleyman BAŞTÜRK	Faculty of Engineering and Natural Science, Altınbaş University	_____
Asst. Prof. Dr. İbrahim KOÇ	Faculty of Engineering and Natural Science, Altınbaş University	_____

I certify that this thesis satisfies all the requirements as a thesis for the degree of Master of Science.

Approval Date of Institute of Graduate Studies:
____/____/____

I hereby declare that all information in this document has been obtained and presented in accordance with academic rules and ethical conduct. I also declare that, as required by these rules and conduct, I have fully cited and referenced all material and results that are not original to this work.

Kamal F. Mohammed

DEDICATION

I would like to dedicate this work to my very first teacher, my mother, my first supporter and role model, and my companion throughout the journey and my brothers. Without you, this dream would never come true.

ACKNOWLEDGEMENTS

I might want to offer my thanks to every one of the individuals who have upheld me all through the regularly extended periods of this voyage. I might want to thank my advisor, Asst. Prof. Dr. Suleyman BASTURK for being my compass notwithstanding, when I believed I was lost and being in extraordinary part in charge of the zenith of this work. I might likewise want to thank my supervisor for his supportive exhortation, which incredibly enhanced the nature of this work. Finally, I thank this institution for hosting me during these years, securely earning its place as my home. I am very thankful to my mom and dad, whose values and education motivate me to keep asking questions; to my siblings and family for their infinitely appreciated love and to my country which, although inanimate, keeps me anchored and offers me an example of resiliency.

ABSTRACT

Numerical study of heat transfer aspects in cutting tools made of Al_2O_3, ZrB_2, TiB_2 and TiN

Kamal F. Mohammed

M.Sc., Mechanical Engineering, Altınbaş University,

Supervisor: Asst. Prof. Dr. Suleyman BASTURK

Co-Supervisor:

Date: November 2020

Pages: 58

In this study, the effects of heat transfer and heat flux on cutting tools with materials of Al_2O_3, ZrB_2, TiB_2 and TiN are investigated numerically with the aid of ANSYS fluent software. The inverse heat flux was described by a function that was concluded from the previous studies and User Defined Functions (UDF) was utilized to define the boundary condition of the friction contact area between the inset and the workpiece which is fabricated from the steel. The insert, shim, and the holder experienced by the ambient temperature equals to 300 K at the beginning of the cutting process then the heat flux was applied. The mesh was generated and regimented at the contact area between the insert and the workpiece and the face between the insert and the holder. The numerical model was validated with the previous study. The influence of the machining parameters for example cutting speed and feed rate on temperature has been investigated to indicate the optimum cutting tool and situation. The cutting tool life will be investigated versus the cutting speed for various materials. The results show that Zirconium diboride (ZrB_2) and Titanium diboride (TiB_2) have a temperature less than the aluminum oxide (Al_2O_3) so that the productivity will increase with the diboride materials utilizing as cutting tool. The maximum temperature for aluminum oxide is 1270 K while the Titanium Nitrite achieved 1092 K. The temperature increase is related

to the cutting speed. The lowest temperature was measured at a cutting speed of 180 m/min, while the maximum temperature has been obtained at a cutting speed of 220 m/min. The optimum cutting condition has been obtained with TiN cutting tool material at 180 m/min cutting speed and 0.138 mm/rev feed rate. Titanium diboride (TiB_2) materials achieved the maximum cutting tool life comparing to other materials.
Keywords: cutting tool, diboride material, insert, temperature distribution, heat flux, tool life.

Özet

Al_2O_3, ZrB_2, TiB_2 ve TiN'den yapılmış kesici takımların ısı transferi yönünden sayısal çalışması

Bu çalışmada, ısı transferi ve ısı akısının Al_2O_3, ZrB_2, TiB_2 ve TiN malzemelerden üretilmiş kesici takımlar üzerindeki etkileri ANSYS sonlu elemanlar analizi programı yardımıyla sayısal olarak araştırılmıştır. Ters ısı akısı, önceki çalışmalardan sonuçlanan bir fonksiyonla tanımlanmış ve iç kısım ile çelikten imal edilen iş parçası arasındaki sürtünme temas alanının sınır durumunu belirtmek için kullanıcının belirlediği fonksiyonlar (UDF) kullanılmıştır. Kesici uç, şim ve tutucunun deneyimlenmiş ortam sıcaklığı, kesme işleminin başlangıcında 300 K sıcaklığa eşit olup daha sonra ısı akısı uygulanmıştır. Ağ, iç kısım ile iş parçası arasındaki temas alanında ve iç kısım ile tutucu arasındaki yüzde oluşturulmuştur. Sayısal model bir önceki çalışma ile doğrulanmıştır. Kesici takım ömrü, çeşitli malzemeler için kesme hızına karşı belirlenmiştir. Sonuçlar, Zirkonyum diborid ve Titanyum diborid'in alüminyum oksitten daha düşük sıcaklığa sahip olduğunu, böylece kesici takım olarak kullanılan diborid malzemeleriyle verimliliğin artacağını göstermektedir. Alüminyum oksit için maksimum sıcaklık 1300 K iken, Titanyum nitrit için 1100 K sıcaklık elde edilmiştir. Sıcaklık artışı kesme hızına bağlıdır. En düşük sıcaklık 180 m/dak kesme hızında, en yüksek sıcaklık da 220 m/dak kesme hızında ölçülmüştür. Optimum kesme koşulları TiN kesici takımla 180 m/dak kesme hızında ve 0.138 mm/rev ilerleme hızında elde edilmiştir. Titanyum diborid (TiB_2) malzemeler, diğer malzemelere kıyasla maksimum kesme takımı ömrüne ulaşmıştır.

Anahtar Kelimeler: Kesici takım, diborid malzeme, insert, sıcaklık dağılımı, ısı akısı, takım ömrü.

TABLE OF CONTENTS

Pages

ABSTRACT ..... **vii**

LIST OF TABLES ..... **xii**

LIST OF FIGURES ..... **xiii**

LIST OF ABBREVIATIONS ..... **xvi**

LIST OF SYMBOLS ..... **xvii**

1. INTRODUCTION **1**

1.1 MACHINING PROCESS 1

1.2 CUTTING PROCESS 1

1.2.1 Cutting Tool Shape and Formation 2

1.2.2 Cutting Tool Types 3

1.2.3 Required Properties of Cutting Tool Materials 4

1.2.4 Cutting Tool Materials Types 5

1.2.4.1 Tool steels 5

1.2.4.2 High speed steels 5

1.2.4.3 Carbides 5

1.2.4.4 Multilayered coatings 6

1.2.4.5 Ceramics: 7

1.2.4.6 Diamond 7

1.2.4.7 Cubic boron nitride (CBN): 7

1.2.5 Sources of Heat Generation in Metal Cutting 8

1.3 TOOL LIFE 9

1.3.1 Methods for Tool Life Measurements: 10

1.3.2 Factors Affecting Tool Life: 10

1.3.3 Wear Curves and Tool Life 11

1.3.4 Tool Life Method 11

2. LITERATURE REVIEW 13

2.1 INTRODUCTION 13

2.2 MACHINING PARAMETERS EFFECTS ON TEMPERATURE DISTRIBUTION ... 13

2.3 CUTTING SPEED EFFECTS ON CUTTING TOOL LIFE 27

2.4 THE NOVELTY OF THE STUDY 29

3. NUMERICAL STUDY 31

3.1 MATERIAL SELECTION 31

3.2 GEOMETRY OF THE TOOL 31

3.3 NUMERICAL METHOD 33

3.3.1 Physical Model 33

3.3.2 Meshing 33

3.3.3 Governing Equations 35

3.3.4 Boundary and Initial Condition 37

3.4 VALIDATION 37

4. RESULTS AND DISCUSSIONS 40

4.1 TEMPERATURE VARIATION WITH TIME 40

4.2 INFLUENCE OF CUTTING CONDITIONS IN THE TEMPERATURE ESTIMATION 43

4.2.1 The Effect of Cutting Speed on the Temperature 43

4.2.2 The Effect of Feed Rate on the Temperature 44

4.2.3 Influence of Cutting Speed on the Cutting Tool Life 44

4.3 TEMPERATURE DISTRIBUTION 46

5. CONCLUSION 52

6. FUTURE STUDY 53

REFERENCES 54

LIST OF TABLES

Pages

Table 3.1: Specifications of the cutting tool materials. 31

Table 3.2: properties of workpiece and holder materials..... 31

Table 3.3: Error percentage of average temperature and heat flux. 35

Table 3.4: Constants parameters C and n for various materials. 36

LIST OF FIGURES

Pages

Figure 1.1: Photograph of cutting tool [1]. 3

Figure 1.2: Sources of heat generation in metal cutting [2]. 8

Figure 1.3: Distribution of heat generated in machining to the chip, tool, and workpiece [21]. 9

Figure 1.4: Typical tool rate curves for flank wear: (a) as a function of time and (b) as a function of cutting path [3]. 11

Figure 2.1: Influence of thermal number on the average interface temperature for natural restricted contact [8]. 15

Figure 2.2: Variation of average interface temperature with cutting speed and feed per revolution [9]. 16

Figure 2.3: The measured temperature at the defined locations of the cutter without heat pipe cooling [20]. 20

Figure 2.4: Heat dissipation from cutting tool by conduction to holder [35]. 26

Figure 2.5: Impact of cutting speeds at the mean and maximum temperatures in the shear and friction zones [38]. 27

Figure 2.6: The influence of cutting speed and feed rate on temperatures [41]. 28

Figure 3.1: Three-dimensional model of the geometry of insert and cutting holder. 32

Figure 3.2: The dimensions of the cutting tool with insert and cutting holder. 32

Figure 3.3: Dimensions of the insert and contact area between the inset and the workpiece. 33

Figure 3.4: 3D of mesh generation grids. 34

Figure 3.5: Elevation view of the grid generation. 34

Figure 3.6: Mesh generation of the insert. 35

Figure 3.7: Comparison between the numerical results and the previous studies of Brito [27] and Ferreira [32] for the heat flux. 38

Figure 3.8: Comparison between the numerical results and the previous studies of Brito [27] and Ferreira [32] for the average temperature. 39

Figure 4.1: The average temperature of the contact area during the cutting for various materials. 40

Figure 4.2: The maximum temperature of the contact area during the cutting for various materials. 42

Figure 4.3: The minimum temperature of the contact area during the cutting for various materials. 42

Figure 4.4: The relation between the temperature and the cutting speed of the cutting tool. 43

Figure 4.5: The relation between the temperature and the feed-rate FR of the cutting tool for TiN. 44

Figure 4.6: the relation between the cutting tool life and cutting speed for various materials. 45

Figure 4.7: Contour of the temperature at 5 seconds. 46

Figure 4.8: Contour of the temperature at 20 seconds. 48

Figure 4.9: Contour of the temperature at 30 seconds. 49

Figure 4.10: Contour of the temperature at 40 seconds. 50

Figure 4.11: Contour of the temperature at 50 seconds. 51

LIST OF ABBREVIATIONS

Al_2O_3	:	Aluminum oxide
ZrB_2	:	Zirconium diboride
TiB_2	:	Titanium diboride
TiN	:	Titanium nitrite
SEM	:	Scanning Electron Microscope
UDF	:	User Defined Function
AB	:	Shear-plane
BC	:	Interface of the tool-chip
BD	:	Interface of tool-workpiece
CBN	:	Cubic Boron Nitride
LMI	:	Laser Melt Injection
HVG	:	Hyper Velocity Gun

LIST OF SYMBOLS

t	:	Time (s)
T	:	Temperature (K)
k	:	Thermal conductivity (W/m. K)
C_p	:	Specific heat (J/kg. K)
v	:	Cutting velocity (m/min)
$\dot{q}$	:	Heat flux (W/m^2)
σ	:	Boltizman constant
FR	:	Feed-rate (mm/rev)
s	:	Second (s)
ρ	:	Density (kg/m^3)
φ	:	Radiative source term
ε	:	Emissivity

1. INTRODUCTION

Metal cutting at the tool – chip interface is characterized by intense contact loading. The coupling between the thermal and mechanical loads leads to a failure of the device, especially under dry conditions configuration, that is to say, machining without lubrication. In order to preserve the structural integrity of the product cutter, efficient heat transfer and temperature rise at the chip-tool interface play an important role. In general, because of the high contact strain, high temperature, and strong friction applied to the tool-chip interface during the machining process, interface parameters are exceedingly difficult to approximate by experimental means alone. In order to forecast tool wear, analytical approaches may offer substantial solutions.

1.1 MACHINING PROCESS

Machining is one of the various processes in which a piece of raw material is cut through a controlled material removal process to a desired final shape and size. The processes that have this common theme, controlled material removal, are often commonly referred to as subtractive manufacturing, unlike processes of controlled material addition, known as additive manufacturing. Exactly what the controlled component of the term entails will vary, but it almost always requires the use of machine tools. Machining forms part of the manufacturing of many metal goods, but may also be used with materials such as wood, rubber, ceramic and composite materials. An individual is called a machinist who specializes in machining. A room, house, or business is called a machine shop where machining is performed. Most of modern-day machining is carried out by computer numerical control (CNC), in which the movement and operation of mills, lathes and other cutting machines is controlled by computers. As the CNC system works unmanned, this increases productivity and thereby decreases labour costs for machine shops.

1.2 CUTTING PROCESS

Cutting is the division or opening, by the application of an acutely guided force, of a physical entity into two or more parts. The knife and saw, or the scalpel and microtome, are commonly used for cutting implements in medicine and science. However, if it has a hardness that is sufficiently larger than the object being cut, and if it is applied with sufficient force, any sufficiently sharp

object is capable of cutting. When applied with adequate intensity, even liquids may be used to sever objects.

Cutting is a phenomenon of compression and shearing and only occurs when the total stress generated by the cutting implement exceeds the ultimate strength of the object's material being cut. The tension produced by a cutting device is directly proportional to the force with which it is applied and inversely proportional to the contact area. Therefore, the narrower the region (i.e., the sharper the tool for cutting), the less force it requires to cut anything. Cutting edges are usually seen to be thinner for cutting soft materials and sharper for tougher materials. This progression is seen from kitchen knife to cleaver, to axe, which is a balance between the thin blade's simple cutting action vs. power which the thicker blade's edge toughness.

1.2.1 Cutting Tool Shape and Formation

As shown in Figure 1.1, the cutting instrument consists of an insert, shim, clamp, clamp screw, and tool holder. Inserts are independent cutting instruments of varying shapes with many cutting sides. Thus, a square insert has eight cutting edges, and a triangular has six cutting edges. Inserts are available with different locking methods and are normally clamped on the tool shank, which is the preferred option since. It is indexed (rotate in it is holder) after one cutting edge is worn such that another edge can be used. The definitions of the cutting tool geometrical parameters, which are also valid for other types of cutting, but with some adjustments related to their features, are examined on the example of a turning tool. Straight turning cutter consists of the cutting part with the corner 1 and shank. Surface 2, upon which the chip flows, is called rake surface or face and the other two surfaces facing the transient surface and the machined surface are called the major flank 3 and the minor flank 4 respectively. The intersection of the face with major and minor flanks forms the major cutting edge 5 and the minor cutting edge 6 respectively. For defining, specifying and measuring angles of a cutting tool in sharpening, the two reference planes are used: the cutting-edge plane and the reference plane. The cutting-edge plane passes through the major cutting edge, tangent to the transient surface and cutting velocity vector. In straight turning the reference plane contains the vectors of the axial and radial feed; it is perpendicular to the cutting velocity vector and the cutting-edge plane. In the particular case, this plane coincides with the base of the tool shank.

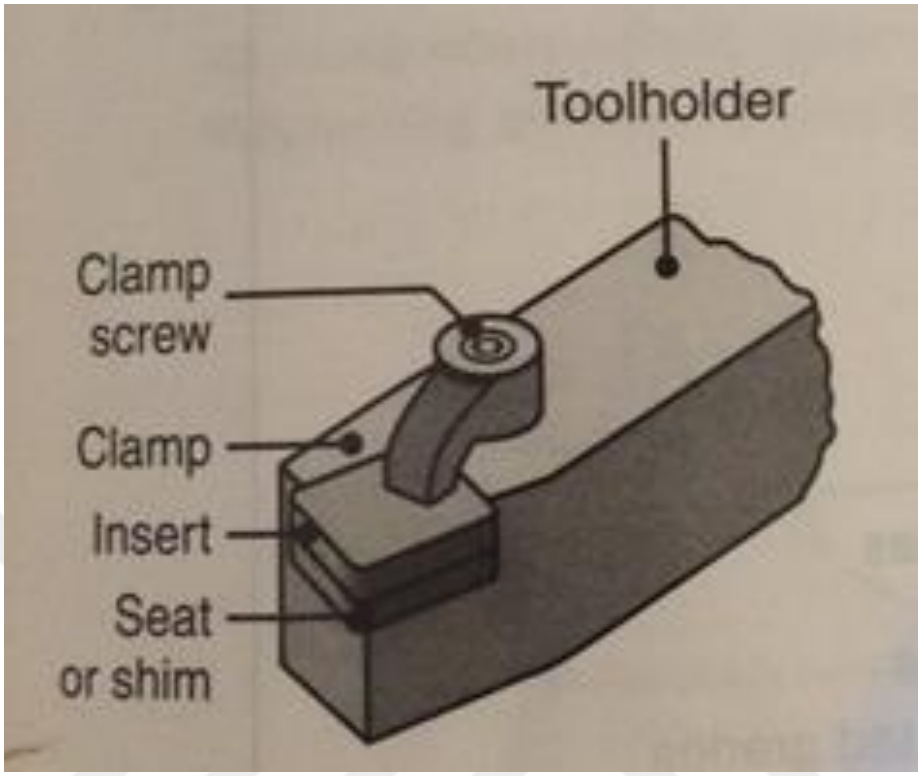

Figure 1.1: Photograph of cutting tool [1].

1.2.2 Cutting Tool Types

Reamer: A reamer is a device by which the hole opened by a drill is filled according to the required precision. The blade material includes diamond / CBN, high-speed instrument steel, and cemented carbide, similar to the cutting tool. The number of cutting edges varies from one to many, depending on the hole diameter and application. In the staggered reamer, the blade is broken into several stages, supporting multiple processes with a single reamer. Drill: A drill is a cutting tool with a cutting edge at the tip and a discharge chip groove in the body that pierces a hole in a workpiece.

Between cutting instruments, it is the most common method, with different shapes and forms for use, from the one used at home to the one for special manufacturing. Milling machines: A milling tool is a common term for machines with several cutting edges on a disc or cylindrical body's exterior surface or end face; when rotating, it cuts the workpiece. It is primarily used in the milling machine and the machining center; diamond / CBN, high-speed tool steel, and cemented carbide are part of the blade material. An end mill is a form of milling method, too. End-mill: An end-mill

is a common term for shank style milling on the outer surface and the end face with a cutting point. Broach: A broach is an instrument for machining the surface of a workpiece or the inner surface of a hole in a broaching machine in which multiple cutting edges are placed around the axis of the bar-like outer diameter of the main body in order of dimension.

1.2.3 Required Properties of Cutting Tool Materials

The cutting tool materials used for the manufacture of cutting tools, must meet the following requirements:

- High hardness, more than 3...4times higher than the hardness of the workpiece material
- Hot hardness, i.e. The ability to maintain the necessary hardness up to a certain temperature
- High wear resistance at elevated temperatures, i.e. The resistance of the cutting wedge to wear
- High strength and dimensional stability of the cutting wedge.
- The material must remain harder than the work material at elevated operating temperatures. The material must withstand excessive wear even though the relative hardness of the tool-work materials changes. The material must have sufficient toughness to withstand shocks and vibrations and to prevent breakage. The cost and easiness of fabrication should have within reasonable limits.

All the currently known tool materials can be divided into the following groups:

- Tool steels
- High-speed steels
- Sintered carbides
- Super-hard materials
- Abrasives.

1.2.4 Cutting Tool Materials Types

1.2.4.1 Tool steels

This is a carbon and low-alloy steels. After water quenching and tempering the hardness of the carbon steel is HRC 61...63. These steels have low cost and high processability, as well as high strength and wear resistance. The main drawback of high carbon steels is their low heat resistance of 200...250°C. To improve the processability and cutting properties the carbon steels are alloyed in small quantities (1...3%) with the alloying elements (chromium, silicon, manganese, tungsten, molybdenum, vanadium, etc.). All low-alloy tool steels due to the high carbon content (0.9...1.1%) have hardness of HRC 61...63 after the heat-treatment, good through hardenability and a somewhat higher hot hardness (up to 250...300°C).

1.2.4.2 High speed steels

High Speed Steel (19265 GOST -73) differ from the tool carbon and low alloyed steels by higher content of the alloying elements, such as tungsten, molybdenum, chromium, and vanadium. As a result of the heat treatment the high speed steels (HSS) have high hot hardness (up to 620°C) and hardness (up to HRC 63...64) and bending strength (σb=3000...3500 MPa). Therefore, the high-speed steel allows cutting speeds of 4...6 times higher than the speed of cutting tools made of tool steels. Due to high toughness the HSS remains one of the most widely used tool materials to present day.

1.2.4.3 Carbides

A composition of the powders of refractory compounds. Tungsten carbides, titanium carbides, tantalum carbides, etc., sintered with binder, mostly cobalt, at high temperatures in a vacuum or controlled atmosphere. The share of the carbide cutting tools is currently about 55%. Due to its high heat stability, hardness and wear resistance the cutting speed for the carbide tools is 4...5 times higher compared to the high-speed tools. However, the bending strength of carbides is significantly (2...3 times) inferior to the high speed steel. The carbides, by its composition and application, are conventionally divided into four main groups:

- Single-component tungsten-cobalt carbide (WC)

- Two- component titanium-tungsten carbide (TC)
- Three component titanium-tantalum-tungsten carbide (TTC)
- Tungsten-free carbides – titanium carbide and carbonatite based.

Heat stability of tungsten carbide grades is 800...850°C. To improve the wear resistance and strength of carbides, the carbide grain sizes are reduced from course to fine and to ultra-fine. Single-component carbides are used in cutting of cast iron, non-ferrous metals and alloys. For cutting of steel and other materials (except titanium) the two component carbides are used. The presence of titanium carbides increases resistance to abrasion on the rake surface of tools. Heat stability of the carbide is 850...950°C. Even greater heat stability (up to 1000°C), strength and resistance to shock loads showed the three-component carbides, which contain tantalum carbide in addition to titanium carbides. International designation of carbides is guided by ISO 513, which divides carbides into the six groups, with relation to the workpiece material, type of the chips produced and other factors. Classification adopted in Russia is based on chemical composition of the carbides. According to ISO all groups of carbides are divided into subgroups, which are indicated by indices: 01, 10, 20... 50. The lower is the index, the thinner is the uncut chip and the higher is the cutting speed the higher is the wear resistance of the tool material. With the index increasing, the feed and depth of cut, as well as tool material strength increase. For example, P 05 denotes carbide used for finishing machining of steels; M 25 is for machining of stainless steels; P 50 is for roughing machining of steels, etc. To increase life of the tools made of carbides and high-speed steels, various wear-resistant single.

1.2.4.4 Multilayered coatings

Such as titanium carbides, nitrides and carbonatites, aluminum oxide etc. gained wide application recently. The optimum thickness of the coating is 6...10 μm for carbide inserts and 2...6 μm for high-speed tools. Thanks to high hardness and wear resistance, chemical inertness to the material and low thermal conductivity of the coatings, it is possible to increase the tool life in 2...5 times and increase the cutting speed by 20...60%. In most cases, the coating is applied by PVD (physical vapor deposition) coating method. The hardness of these coatings at any temperature is higher than that of the coatings obtained by CVD (chemical vapor deposition) method.

1.2.4.5 Ceramics:

Consisting of aluminum oxide Al_2O_3, and produced by melting alumina (bauxite) in electric furnaces. This type of ceramic is also called the oxide ceramic or white ceramic. It has a very high thermal stability (up to 1400...1500°C) and hardness (*HRA* 90 ... 92), greater than that of carbides, allowing to cut metals at 300...600 m/min or higher. The main disadvantages of ceramics are its low bending strength (σ_b=320 MPa), which is an order of magnitude smaller than the bending strength of high-speed steel, and high strength instability. To increase strength the mineral ceramics are introduced with various refractory compounds: oxides and carbides of tungsten, molybdenum, titanium, etc. Thanks to these additions, as well as reinforcement by filamentary single crystals of silicon carbide (whisker-reinforced), black ceramic compared with white ceramic has higher bending strength (σ_b=560...700 MPa), stable properties, but less wear resistance. Recently, new grades of ceramics based on silicon nitride Si_3N_4, the so-called gray ceramics, which bending strength increased to 800 MPa were created. This allows to apply this ceramic not only for finish turning of high strength steels and cast irons, but for milling as well, which is characterized by shock loading. The group of super-hard materials includes diamond (natural and synthetic) and cubic boron nitride (CBN).

1.2.4.6 Diamond

Diamond is the hardest material in nature (4...5 times harder than tungsten carbide) and has high thermal conductivity, low coefficient of friction, low bending strength and low ignition point (800°C). At higher temperatures the diamond is oxidized and graphitized to CO and C. The extreme brittleness of the diamond it greatly limits its use in metalworking. One of the major drawbacks of the diamond is its chemical affinity to iron. Therefore, the natural diamond crystals are not use for cutting of steel, and, thus are used only for finish turning of nonferrous metals and alloys at high cutting speeds.

1.2.4.7 Cubic boron nitride (CBN):

CBN is a synthetic material with a complex diamond-like crystal lattice; it has no natural counterpart. CBN hardness is close to diamond, but its thermal stability is higher, reaching 1200°C. CBN is chemically inert material and, therefore is suitable for cutting of metals of different composition. Due to the high hardness and wear resistance it is used for cutting very hard materials,

hardened steels and even carbides. Polycrystalline cubic boron nitride (PCBN), depending on the composition and manufacturing technology, has bending strength σb= 470...1200 MPa.

1.2.5 Sources of Heat Generation in Metal Cutting

Significant amounts of heat are emitted from the cutting point at three separate source points during machining, as seen in Figure 1.2. The energy dissipated in plastic deformation is transformed into heat by cutting virtually everything, allowing temperature to rise in the cutting field. This will to some extent increase the wear of the instrument, and thus decrease the life of the instrument. In the cutting field, water like this generation is directly linked to plastic deformation and friction between the chip and the unit, the instrument and the workpiece, and the different cutting forces. Since metal cutting requires a significant amount of plastic tension, almost 99% of the heat is transmitted to the chip, cutting tool and workpiece, while more than 1% of the work is deposited as elastic energy. The three heat producing sources are:

1. Shear-plane (AB), where the real deformation of plastic happens.
2. Interface of the tool-chip (BC) due to the tension between the tool and the chip.
3. Interface of tool-workpiece (BD), which appears on the flank surface.

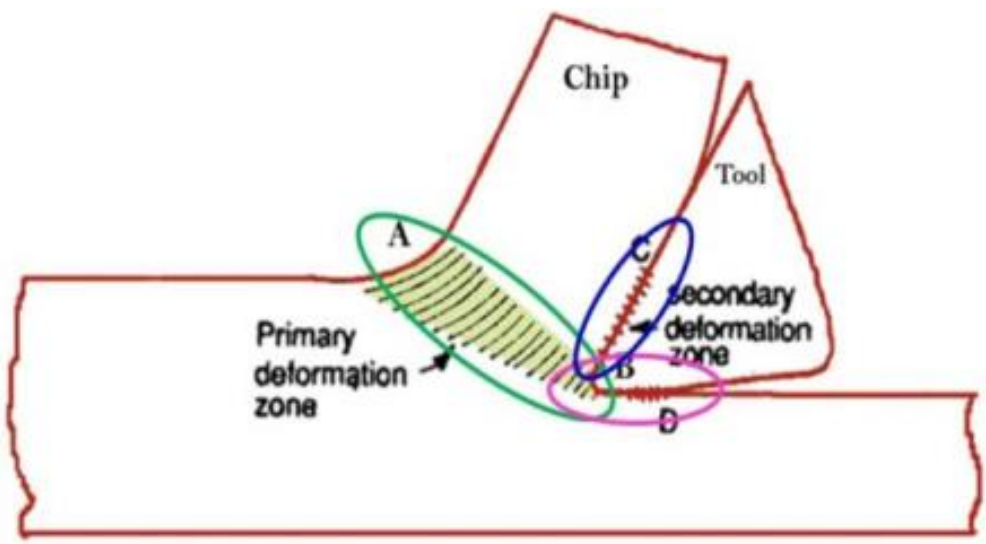

Figure 1.2: Sources of heat generation in metal cutting [2].

Distribution of heat generated in machining to the chip, tool, and workpiece without heat transfer into the surrounding environment is illustrated in Figure 1.3. It is indicated that the higher value of heat transfer into the chip and the rest of the heat go through the cutting tool and the workpiece.

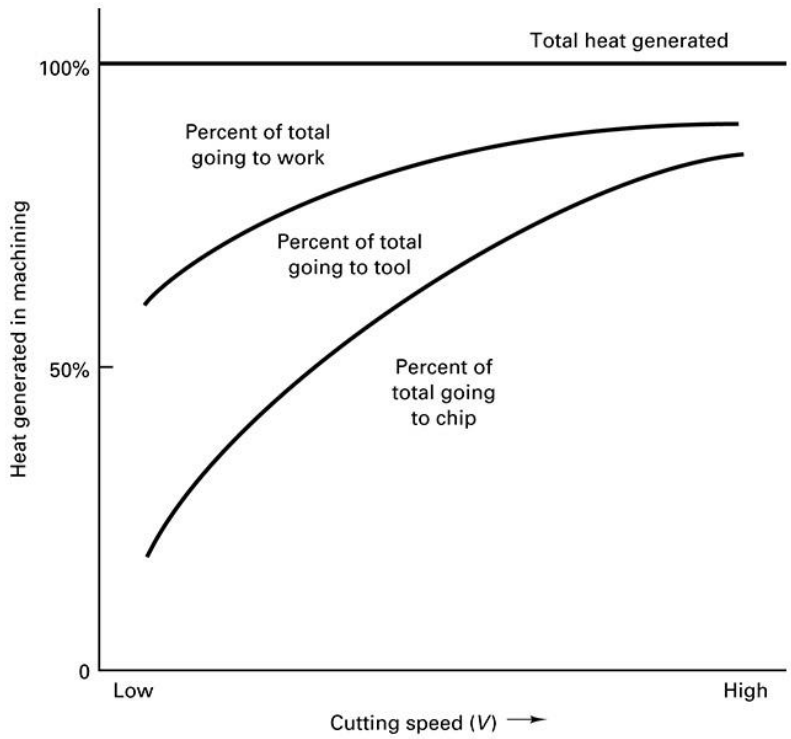

Figure 1.3: Distribution of heat generated in machining to the chip, tool, and workpiece [21].

1.3 TOOL LIFE

The practical existence of every system or instrument. It can work at its expiry, but not effectively. And it's accurate for a cutting instrument as well. The tool loses its content during use, i.e., it gets worn out. The tool loses its productivity as wear increases. So, its life needs to be established and it should be reground for fresh use at the end of its life. It is possible to describe the life of the instrument in various ways:

- The time for two consecutive grinding processes has elapsed.
- The time during which an instrument cut satisfactorily.

- The cumulative time accrued until the malfunction of the instrument takes place.

1.3.1 Methods for Tool Life Measurements:

The most commonly used methods for tool life measurements are following:

- Machining Time:

Elapsed time of operation of machine tool.

- Actual Cutting Time:

The time during which the tool actually cuts.

1.3.2 Factors Affecting Tool Life:

The following factors play an important role in tool life:

- Cutting speed.
- workpiece machine-tool Rigidity system.
- Feed rate and Depth of cut.
- Workpiece grain size.
- Microstructure of workpiece.
- Tool material.
- Workpiece hardness.
- Tool geometry.
- Nature of cutting.
- Type of cutting fluid and its method of application.

The period of cutting by a new or regrinded cutting tool till its failure, or up to the maximum permissible wear limit, is called a tool life. Except time, tool life can be defined as the area of the machined surface, the number of parts, holes, etc. Tool life effects on the cutting process productivity. Thus, in theory and practice of cutting, the tool life improvement is of primal concern.

1.3.3 Wear Curves and Tool Life

The relationship between the sum of flank wear (rake) and the cutting time and the average length of the cutting path is demonstrated by tool wear curves. Using the effects of cutting experiments, these curves are interpreted in linear coordinate systems, where flank wear VBB max is measured after certain time intervals (Figure 1.4(a)) or after a certain cutting path length (Figure 1.4(b)). On such curves, there are normally three distinctive regions that can be observed. The area of main or original wear is the first area. In this area, the relatively high wear rate (increased tool wear per unit time or cutting path length) is explained by accelerated wear of the tool layers weakened during processing or resharpening. The region of steady-state wear is the second region. For the cutting instrument, this is the usual operational area. The third region is referred to as the region of tertiary or rapid wear. In this region, accelerated tool wear is usually accompanied by elevated cutting.

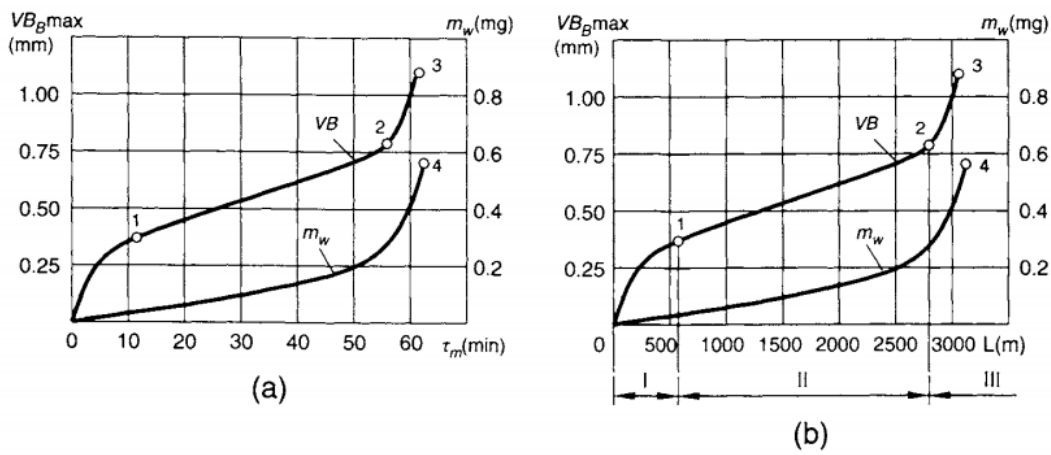

Figure 1.4: Typical tool rate curves for flank wear: (a) as a function of time and (b) as a function of cutting path [3].

1.3.4 Tool Life Method

It is possible to base machinability on the calculation of how long a tool last. When comparing materials that have identical properties and power consumption, this may be beneficial, but one is more abrasive and therefore limits the life of the instrument. The main weakness of this method is that the life of the tool relies on more than just the material it is machining; other variables include material for cutting tools, geometry of cutting tools, state of the unit, clamping of cutting tools,

speed of cutting, feed, and cutting depth. Even, it is not feasible to compare the machinability for one type of instrument with another type of instrument. Economic tool life is the lowest running expense. Tool life for efficiency-the tool's productivity is the highest regardless of the cost of service. A material's machinability ranking seeks to measure the machinability of different materials. It is expressed as a normalized value or ratio. Machinability Rating= (Speed of machining the workpiece giving 60 min of tool life) / (speed of machining the standard metal) In accordance with the Taylor tool life equation, machinability ratings may be used:

$$v\,t^{n} = C$$

where v is the cutting velocity, t is the time in minutes, and C and n are constants.

2. LITERATURE REVIEW

2.1 INTRODUCTION

The high-temperature values disturb the performance and quality of numerous engineering processes such as the machining process in which cutting tool has high temperature. This leads to change tool physical properties and microstructure during machining. The disadvantages of those changes represent in reduction of material resistance of mechanical stresses so that performance and lifespan of cutting tool decrease. The processing impacts increase the operation cost and decrease the products quality. The study of heat flux as well as the temperature at different machining parameters can be useful for efficient cooling systems development and determining the optimum operation parameters.

2.2 MACHINING PARAMETERS EFFECTS ON TEMPERATURE DISTRIBUTION

Valvo et al. [4] studied a multiple method to estimate the temperatures in the ceramic tools cutting process. He evaluated the temperature lines with 3D cutting approach experimentally by applying constant melting point powders dispersed on planes parallel to rake face. Numerical analysis was completed to determine the percentage of heat transferred to the cutting tool during the operation and the temperature distribution of the insert and cutting holder. Temperature distribution was examined with SEM microscopy to confirm the numerical results. The results showed that at cutting speed equals to 11 m/s metal appeared in the fractures of the inserts so that the cutting temperatures exceeded 1540 ^{o}C.

Ay and Yang [5] performed the simultaneous and integrated measurement of temperature distribution through calibration against thermocouples, he used an infrared thermographic system. Using two kinds of tool inserts, four different workpieces were milled to determine the temperature distribution of the carbide inserts under different conditions and how heat transfer can impact the wear of the tool. In addition, at the post-cutting point, there was an optical and electronic microscope used for microscopic inspection of tool surfaces. The results revealed that in ductile fabrics, with a 0.05 mm/rev feed and 0.25 mm cutting depth, the critical value of cutting speeds for the phase of transition from mechanical to diffusion wear is lower at 2 m/s. In the mechanical wear zone, the rate of reduction in tool life is higher and in the diffusion wear zone, it is slower.

Chip geometry may cause a zigzag variation in the temperature of the steady state regarding the rate of material removal for a change in cast iron and copper feed. The research sheds light on the roughness influences of surfaces that are cut with a hard tool and can thus act as the first step in surface machining investigations.

Kharkevich et al. [6] studied the heat flux transfer in the cutting instrument for orthogonal steady-state cutting. In order to determine tool temperature distributions from various heat flux transfer conditions, the process requires an iterative method. The distributions of temperature measured from this approach have been contrasted with the distributions obtained experimentally. A coincidence of the experimental and theoretical temperature distributions meant that the model selected for heat flux was suitable. It was clear that the average temperatures derived from climate simulations, which differ greatly from those derived, were based on experimental measurements. Thus, if precise forecasts are needed, the consequence of the uniqueness of heat flux transfer in the cutting tool must be considered by these models.

Pfefferkorn et al. [7] studied and validated comprehensive thermo-mechanical model for Laser-assisted machining. A transient, three-dimensional heat transfer model that integrates relevant physical characteristics of the processes of heating and material removal has been developed and projections have been matched with surface temperature background measurements for rotating workpieces of cylindrical silicon nitride. The experiments and predictions showed that for the laser-tool traverse distance of this sample, near-laser, quasi-stable conditions are not attainable, thus requiring characterization of the process as time-dependent. As rotational speed rises due to the influence of increasing circumferential advection, the peak temperature at the place of the measurement increases slightly. As the laser power decreases, the laser-tool lead gap decreases and/or the laser / tool transmitting speed rises, the volume of energy deposition decreases within the unmachined workpiece, thus decreasing the temperature.

Grzesik and van Luttervelt [8] researched the thermal effects associated with Multilayers coatings in orthogonal cutting. For given machining specifications, the thermal number used is an essential factor supporting the design of coated grooved tools. The findings revealed that maintaining the contact temperature below the recommended values for the coatings added is most significant. In particular, the avoidance of tension should be based on a professional reduction in contract length. As seen in Figure 2.1, the contact length can also be easily used to monitor the heat flux and

thermal load of the tool-chip interface. The data obtained from these tests can be connected via the Technology Network to an internet database for dry cutting to help the correct choice of coatings at the optimum contact temperature.

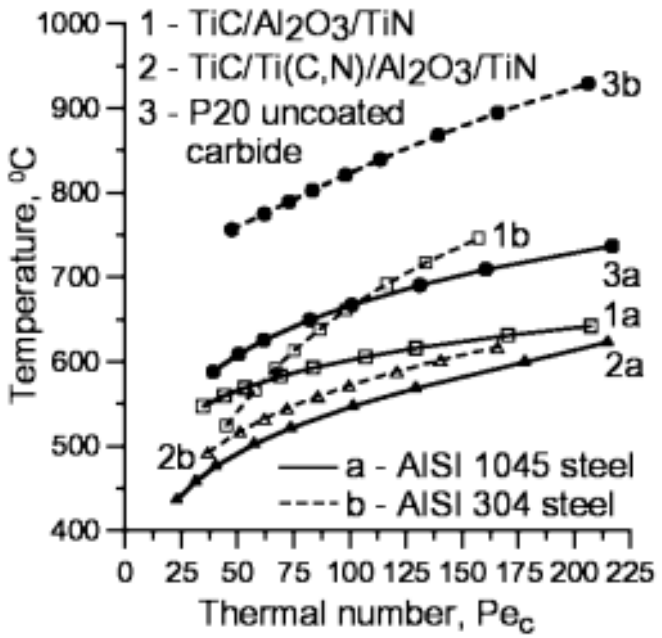

Figure 2.1: Influence of thermal number on the average interface temperature for natural restricted contact [8].

Lazoglu and Altintas [9] predicted the tool and chip temperature in continuous and interrupted machining The findings revealed that with each of these discretized machining cycles, Steady-state chip and tool temperature fields were calculated. Time constants for each distinct machining interval is calculated based on thermal properties and boundary conditions. An algorithm to calculate the transient temperature fluctuations in disrupted turning and milling operations was presented by understanding the steady-state temperature and time constants of the discretized first order heat transfer method. Simulations were conducted under varying cutting conditions for various materials. The findings were well correlated with experimentally determined temperatures for continuous and interrupted machining processes as seen in Figure 2.2.

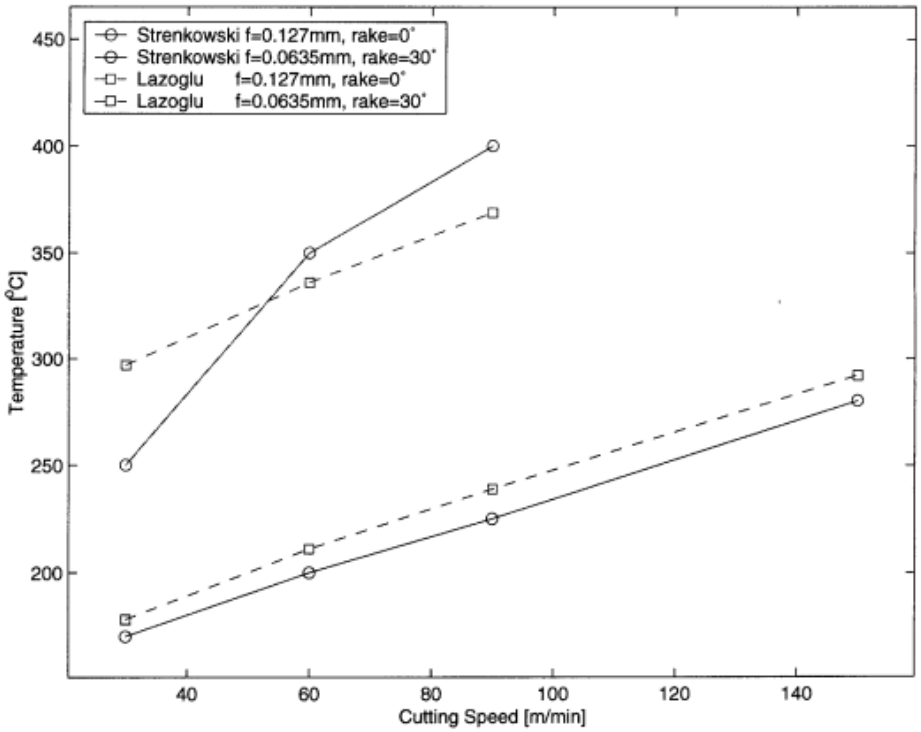

Figure 2.2: Variation of average interface temperature with cutting speed and feed per revolution [9].

Fanghong et al. [3] studied the high-speed milling process with a three-dimensional inverse heat-transfer model to determine the heat flux and temperature distribution on the tool-workpiece interface based on the calculated temperature data. A series of experiments were carried out to validate this model in order to obtain the surface temperature data of the workpiece with the aid of the infrared thermometer and the temperature of the tool-workpiece interface with an integrated artificial thermocouple. The complex properties of cutting temperature have been extensively tested in high-speed aluminum alloy milling. The findings of the computational simulation showed that minor errors occurred when comparing heat flux values derived from the model and from functional experiments. In the high-speed milling of aluminum alloy, a crucial cutting speed occurs. For various cutting conditions, the importance of this critical speed is distinct. If the spindle speed increases, the heat flux flowing through the workpiece increases. The increase in heat flux flowing into the workpiece will decrease when the cutting speed exceeds the critical speed.

Brookes et al. [10] observed under varying laboratory temperatures, the functions of binder phase structure, volume fraction and CBN grain size in the hardness of CBN cutting tools. A variation

in the hardness regulating process is found in the products containing TiC and TiN at temperatures below 0.4 Tm. The change in mechanism is shown to be representative of the brittle-ductile transformation by contrast with evidence from the soft impression technique. This implies that the technique of soft impression is an important instrument that can be used efficiently in conjunction with more established methods. The use of Ito-Shishok in plots for metals and single crystal materials gives strong signs of improvements in the mechanism of deformation. This is not, however, the case with composite materials, such as those used in this work. Further work would be required to determine the activation energies associated with the deformation mechanisms in order to explain the deformation mechanisms which occur in these materials. It will then be possible to compare with the activation energies of the constituent materials and to ascertain the relationship of the constituent parts within these composite materials.

Melkote et al. [11] modeled the cutting tool temperatures in the rotary tool turning of hardened steel. A good agreement was found between the temperature distribution predicted and measured along the cutting edge. The model can, therefore, be used to provide a good understanding of the cutting temperature during a rotating tool cycle. Due to the spinning motion, the self-propelled rotary tool process provides a cooling cycle for the cutting edge and could, therefore, have a positive effect on lowering the temperature of the instrument. Results provided in this investigation support this statement and this drop in temperature is promising for future studies of the rotary tool's wear behavior. Battaglia et al. [12] presented an analytical solution of heat diffusion in a coated tool, to model and to quantify the thermal influence of a coating, without considering its tribological influence. Moreover, the heat flux entering into the substrate is analyzed taking into account the thermophysical properties of the deposit and its thickness. It was found out that the tribological phenomena at the tool-chip interface is the key reason why variations in the heat flux transferred to a substratum are clarified.

Grzesik [13] used the AdvantEdge Lagrangian finite element code to create a plane-strain orthogonal metal cutting model of a coupled thermo-mechanical finite element with continuous chip forming generated by uncoated plane-faced and differently coated carbide instruments. The results of the FEM and empirical simulations, for both uncoated and three-layered coated materials, have been shown to have very appropriate and mechanically checked tests for cutting temperature values and distributions. However, by changing the friction parameter and heat

partition to coated instruments with actual thicknesses, the optimal result can possibly be obtained (in this study, they were based on vendor data and not on calculation using, for example, microscopy scanning. The simulations of finite elements were conducted to show the presence and localization of the secondary shear zone and workpiece. Also, the substrate under the thin coating is visibly cooler in comparison to uncoated tools.

Filice et al. [14] used an arbitrary Lagrangian-Eulerian approach to model orthogonal cutting process and numerical simulations, experimental experiments were performed to classify cutting forces and internal tool temperatures. A mild steel was cut using an uncoated tool (WC) as well as a coated tool (TiN). A consistent model of the global heat transfer coefficient was developed at the tool-workpiece interface based on both experimental and simulative results, as a function of local pressure and temperature.

Arif et al. [15] studied laser treatment of the cutting tool for cemented tungsten carbide. Using the FEM ANSYS code, the production of thermal stress in the instrument is modelled and numerically predicted. An experiment is carried out during the laser treatment process to analyses the structural changes in the tool material. In the region next to the surface area, the temperature gradients in titanium and tantalum carbides are found to be greater than in tungsten carbide. Due to the broad temperature gradient, thermal expansion and consequent thermal strain creation results in excessive von-Mises stress levels in this region. In the tungsten carbide example, the magnitude of the stress level is lower than that of titanium and tantalum carbides. In the high stress concentration zone, crack formation is possible. This state is also observed from the experiment; in this situation, extended cracks are caused over the treated surface.

Kountanya [16] investigated transient instrument temperatures for disturbed machining systems. Heat convection from outside surfaces was part of the functional solution strategy for the Green. The results revealed that modulation decreased the cutting temperature more dramatically at a higher modulation level. Heat conduction over convection into the atmosphere dominated the system, however. It was observed that the instantaneous uncut chip thickness lags at the peak temperature, meaning that modulation would potentially alter the thermal softening of the cutting instrument in continuous cutting without a concomitant decrease in the rate of material removal. The same model of tool temperature applied to face molding indicated that only at the exit of the cut was the highest temperature. There have been deliberately designed hard-facing studies that

differ the magnitude and length of the disruption. The valuable results of lower temperatures due to a minor disruption is indicated by data on tool life. Carvalho et al. [17] studied the effects of heat in cutting tools, taking into account the difference in coating thickness and heat flux. The K10 and the diamond substrates were used with TiN and Al_2O_3 coatings. The numerical approach makes use of the program ANSYS. Boundaries and constant physical thermal conditions. The properties of the solids involved in the numerical analysis are known. The experiments are used to test the suggested technique. After a continuous cut, the TiN and Al_2O_3 coatings did not produce satisfactory results. The heat flux for the 10 (μm) TiN and Al_2O_3 coatings showed a marginal reduction.

Noor et al. [18] studied laser treatment of the cutting tool for cemented tungsten carbide. Using the FEM ANSYS code, the production of thermal stress in the instrument is modelled and numerically predicted. An experiment is carried out during the laser treatment process to analyses the structural changes in the tool material. In the region next to the surface area, the temperature gradients in titanium and tantalum carbides are found to be greater than in tungsten carbide. Due to the broad temperature gradient, thermal expansion and consequent thermal strain creation results in excessive von-Mises stress levels in this region. In the tungsten carbide example, the magnitude of the stress level is lower than that of titanium and tantalum carbides. In the high stress concentration zone, crack formation is possible. This state is also observed from the experiment; in this situation, extended cracks are caused over the treated surface. The findings of XRD suggest that nitride compound formation occurs in the laser-treated area. Cobalt molten flux from the soil below to the free surface is filled by the partly evaporated area on the surface. This increases the concentration of cobalt on the soil.

Noor et al. [19] studied the dry cutting or dry machining has become an ever more necessary approach; no coolant or lubricant is used in dry machining. This paper addressed the impact of dry cutting on cutting force and tool life while using two separate coated carbide cutting tools (TiAlN and TiN / MT-TiCN / TiN) in the aerospace materials machining. The surface-response method has been used to minimize the number of experiments. TiAlN Swarm Optimization models have been developed to optimize the machining parameters (cutting speed, federate, and axial depth) and to obtain the optimal cutting force and durability. Compared with TiN / MT-TiCN / TiN, it is found that carbide cutting tool coated with TiAlN worked better in dry cutting. On the other side,

using 100 percent water-soluble coolant, TiAlN performed higher. The cutting tool still needed lubricant to support the heat transfer from the workpiece because of the high temperature created by the aerospace materials.

Chen et al. [20] tested a cooling method for a heat pump to decrease the cutter 's temperature Through the cutting test, the dry turning temperature of AISI-1045 steel at the specified cutter locations was obtained. The finite-difference approach and an inverse procedure were used to determine the tool-chip interface temperature. It has been observed that the tool-chip interface temperature and effective heat flux of the cutter would increase with the rise in cutting speed. The tool chip interface temperature may be lowered via the heat pipe cooling. The temperature decrease was more apparent at greater cutting speeds. The calculated temperature at the specified positions of the cutter without heat pipe cooling as shown in Figure 2.3.

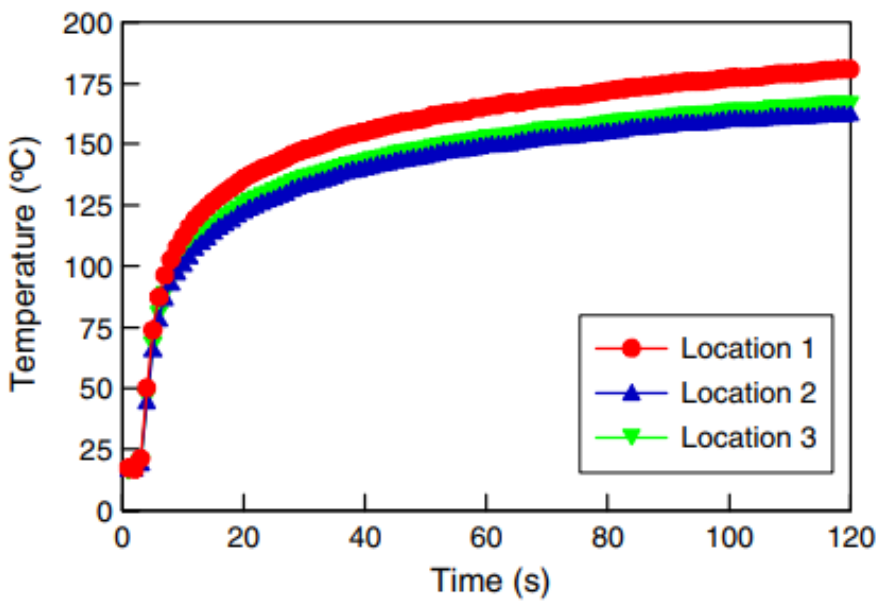

Figure 2.3: The measured temperature at the defined locations of the cutter without heat pipe cooling [20].

Kálazi et al. [21] measured the machinability (after making a cutting tool from it) and also the efficiency of a steel matrix (TiW) C reinforced surface nano-composite developed by the in situ Laser Melt Injection (LMI) process on a cheap steel matrix as a cutting tool. The results showed that the surface nano-composites of Steel-matrix (105WCr6 steel) with (TiW) C micron-sized and (FeW) 6C nano-sized carbide precipitates were produced with subsequent heat treatment by in situ laser melt injection technology. The material produced has all the properties that need to be

classified as cutting material. Our in situ LMI technology is an alternative technology to the processes of PVD which CVD and can be used to improve / increase low-alloy steel performance. The machinability of a cubic boron nitride (CBN) wheel for the LMI nano-composite was found to be lower, but still reasonable compared to the initial matrix. After grinding the LMI nano-composite sample, the surface of the CBN wheel was found polluted by Ti. The following optimum cutting conditions are recommended in order to reduce grinding wheel surface contamination: V = 25 m/s, vf = 1–2 m/min, f = 0.01–0.02 mm/pass. Compared to the original Hyper Velocity Gun (HVG) matrix, cutting instruments constructed from LMI nano-composite by the CBN wheel were found to have greater wear resistance and longer tool life against a C45 steel workpiece. The LMI nano-composite material also produced less cutting power compared to the original HVG steel under equal cutting conditions.

Martan and Beneš [22] presented an experimental study of thermal conductivity and volumetric specific heat of different coatings in the range from room temperature to 500 ◦C. The coatings under investigation were TiN, TiAlCN, TiAlN, AlTiN, TiAlSiN and CrAlSiN. The thermal properties were measured using the pulsed photo-thermal radiometry method. The thermal conductivity of the coatings under investigation varied from 2.8 to 25 (W/m. K) and increased with the rise in temperature. The lowest thermal conductivity was observed for the CrAlSiN coating. Haddag and Nouari [23] studied the wear and heat transfer analyses in dry machining based on multi-steps numerical modeling and experimental validation. It has been shown that this is not necessary only with this thermomechanical calculation to obtain heat diffusion into the insert up to embedded thermocouples within acceptable Processor time. The measurement of the thermal load applied to the tool rake face was made possible by using the contact strain, interface sliding velocity, and contact area obtained from the first stage of the calculation. The thermal analysis carried out with the third stage FE model allows the temperature and heat flux fields in the insert to be obtained and their evolution over a couple of seconds of cutting time (approximately 5 s). The cutting duration of the machining test corresponds to this moment.

Ogawa et al. [24] used the See beck effect that happens between a carbon fiber and a tool material, the cutting point temperature was determined and then the impact of a cutting speed on the temperature of the cutting point was calculated. Secondly, using the embedded K-type thermocouple in the work-piece, the temperature transition within the surface layer of CFRP is

determined. When laminating the prepregs, these K type thermocouple wires were embedded and cured in the autoclave for the development of the CFRP layer. Since the thermal conductivity of the CFRP is very low (i.e. 1.0 W/m K) relative to other metals, the transformation of the CFRP cutting temperature varies radically from that of metals. To explain the surface defect created by the cutting operation, the machined surface was also examined by the scanning electron microscope (SEM). The results showed that CFRP plate milling was performed using solid cemented carbide endmill and temperature measurements using three types of measurement methods, namely cutting point temperature measured by the tool-work-piece thermocouple method, endmill surface temperature measured with an infrared thermograph camera, and machined surface layer temperature measured by the tool-work-piece thermocouple method. This pattern depends on the low CFRP thermal conductivity and the change for intermittent cutting in the time period of the milling process. At the cutting speed of 300 m/min, the measured temperature did not reach the glass-transition temperature of the matrix resin. When inspecting the machined surface by SEM, the matrix resin of the machined surface was not disrupted, even though the cutting speed was as high as 300 m/min. The effect of the temperature elevation at the cutting point on the machined layer remains minimal and slight at such high cutting speeds. As a consequence, it was proposed that high-speed cutting of up to 300 m/min on CFRP milling was acceptable in terms of productivity and machining quality under the cutting conditions used.

Cheng et al. [25] studied the temperature distribution with a cooling system in a smart cutting tool process by measuring the cooling fluid temperature at the inlet and outlet passes. They investigated the efficiency of the micro-cooling construction and the possibility of measuring and controlling the cutting temperature experimentally and numerically. The results showed that the increase of the flow rate leads to a decrease in the resolution of the tool as a temperature sensor. It is indicated that there is a high accuracy with utilizing the numerical prediction model. The suggested micro-internal structure decreases the cutting tool temperature during the process. The new design and cooling solution are suggested for machining of different materials such as titanium and composites. Deiab et al. [26] studied investigated the temperature distribution on the cutting insert with cooling by dry air at room temperature numerically. Minimum quantity of lubrication of the cutting tool as internal cooling studied in this study. Results showed that increasing the velocity of air, forced convection can be achieved and simulated to study the tool temperature distribution. In the metal cutting process to design a CFD model, conduction and convection are treated as

major heat transfer modes. However, there is a need to explore the role of radiation heat transfer mode in the metal cutting CFD simulations.

Carvalho et al. [27] investigated the temperature field in the insert, shim, and cutting-holder and the heat flux estimation at the cutting interface. A significant improvement in the technique to estimate the heat flux and temperatures in a machining process was presented in this work. The use of COMSOL for the numerical solutions of differential equations that control the physics is effective. It is possible to adjust any boundary conditions and model the geometry.

Guo et al. [28] examined the dry cutting and cutting fluid with dissimilar fluid pressure (pouring, 3-6 MPa) for CGI machining to explore the impact of fluid pressure on wear of the tool at different cutting speeds (100-300 m/min). To explore the better cooling and lubrication results, the cutting fluid is jetted directly over the race face and flank face of the cutting instrument. Wear instrument morphologies that have been studied using a 3D view device or SEM. Influences of difference in fluid pressure on cooling and cutting fluid lubricants in machining are discussed. The findings revealed that the fluid's high-pressure jetting along the rake face would also minimise flank wear. However, the wear-reducing effect of high-pressure jetting along the rake face on the flank side of the instrument is weaker, close to that of high-pressure jetting along the flank face.

Di et al. [29] investigated in end milling taking into account the real friction condition on the tool-chip interface and the temperature lowering process, a new analytical model for predicting the cutting tool temperature. Both the computer simulation using the suggested analytical model and the physical cutting experiment was conducted with separate cutting parameters, and the two findings indicate strong agreement. The experimental findings show that the temperature of the instrument increases with the feed per tooth but decreases with the speed of cutting. In order to avoid unnecessary tool wear in end milling, the current theoretical model for cutting tool temperature estimation can be further improved and then used to improve the cutting state. A better litter than high-pressure fluid cutting jetting along the flank face of the cutting tool, high-pressure fluid cutting jetting along the rake face has a beneficial effect on minimising the rake face tool. The key method of carrying a tool on the rake and flank face is chipping and adhesive wear if no cutting fluid is used in CGI machining. Abrasion influences the wear on the rake and flank face of the cutting tool while high-pressure cutting fluid is used. High pressure fluid cutting cooling is a

heat convection forced loop that is determined by fluid velocity, fluid pressure, fluid density, and other parameters.

Pabla et al. [30] suggested a number of measures and techniques for improved machinability of Ti_6Al_4V alloy. A variety of steps and strategies for enhancing Ti_6Al_4V alloy machinability have een proposed. In accordance with technological and economic considerations, the most effective steps and strategies are inferred as follows: low thermal conductivity and high chemical reactivity with the cutting tool are the most influential criteria for limiting Ti_6Al_4V machinability. In Ti_6Al_4V machining, the cutting tool is found to wear equally at high cutting speeds at both the flank and crater due to high heat accumulation at the tool tip and adhesion to the serrated chips, respectively. Due to the absence of elevated cutting temperatures at the tool chip interface, crater wear is observed to cease at lower cutting rates. The most fitting are the WC instruments with 6 percent cobalt as a binder with a grain size between 0.8 and 1.4 μm. While diamond inserts perform better in chemical inertness than CBN instruments, WC tools make them the choice for machining titanium alloys due to their satisfactory low and medium speed performance as well as their cost-effectiveness. Although the Ti6Al4V workpiece reaction with the WC cutting tool results in a degradation in the life of the tool due to the accumulation of carbides, the inclusion of nitrides during machining is favoured for decreased wear of the tool. Thus, for high-speed machining of Ti_6Al_4V alloys, coated WC tools are favoured, with TiAlN, AlTiN, AlCrN, NbN and TiAlSiN coatings suggested for better tool life and increased wear resistance. Both higher and lower thermally conductive coatings than Ti_6Al_4V was considered to boost tool life, taking into account the thermal conductivity of coating materials. It is proposed to change multilayer coatings with high adhesion content as the lower layer and rough and durable content as the upper layer. Therefore, a variety of conflicting hypotheses prevail that need to be justified concerning different cutting conditions for the correct wear process. It is important to create a more appropriate coating that will help mitigate sudden tool loss. Cryogenics are recommended as pre- and post-coating treatment strategies for extending tool longevity. Due to improved microstructure and uniform grain distribution, cryogenic treatment of the tool material before and after coating has resulted in improved wear resistance and mechanical properties. It has resulted in the development of a more stable microstructure in the case of WC instruments, i.e. the Ø process, refining of particle boundaries and increase of thermal conductivity. The lubrication effect of LN_2 as well as rapid

heat travel was considered to be useful in increasing the life of the instrument in cryogenic machining.

Yang et al. [31] investigated the heat transfer and flow shape of high-speed cutting machining with viscous coolant fluid and air and compared the temperature gradient in the two cases. The results showed that the temperature gradient increase with the rise of Pr number with the coolant fluid comparing to natural air convection. They finished the heat transfer model that can be useful for understanding cooling process characteristics.

Magalhães et al. [32] investigated the highest, minimum, and average temperatures for the contact area between the ship and the insert. For validation of the results, comparing the heat flux of this study and the heat flux of other works was applied. They studied the temperature variation of coated carbide tools throughout the thicknesses. The results indicated that the coated carbide cutting tool presented higher temperatures for the flux contact area than the uncoated carbide tool. It is indicated that the increase of thicknesses has more effect on the cemented carbide . It can be concluded that the Al_2O_3 coating is better than TiN because of the low thermal conductivity value and protective for the cutting tool concerning heat. Cutting tool and increase the temperature of the contact area. The coated and uncoated carbide cutting tools presented a peak difference in the cutting region of 12.7 °C for the TiN and 75.5 °C for the Al_2O_3.

Molnar et al. [33] investigated a method to determine the contact length during the cutting process experimentally and numerically. Theoretical expressions with orthogonal cutting test and FE simulations were introduced. The results showed a good agreement between the FE simulations and the Lee and Shaffer model of contact length based on the Minimum Energy Principle (MEP) shear angle model. Parida and Maity [34] discovered an easy and simple model for heating the work-piece by flame heating with study. They studied the influences of speed of cutting, feed rate, and temperature on cutting force and specific energy. Nickel base alloy was examined in room temperature and high-temperature conditions during the turning process with the aid of deform software. A respectable correlation between the numerical and experimental results was achieved. The results indicated that the energy of performing the machining process and cutting force in the case of hot processing is less than the case of room temperature conditions. Therefore, the shear stress with heating reduce gradually.

Vajdi et al. [35] studied the heat transfer, temperature distribution, and maximum temperature for cutting processes in diboride-based materials such as HfB_2, ZrB_2, and TiB_2 as well as HfB_2–20 vol% SiC, ZrB_2–20 vol % SiC and TiB_2–20 vol% SiC composites. The results indicated that the rising slope of temperature for HfB_2 is higher than those of ZrB_2 and TiB_2 where the lowest maximum temperatures were achieved for ZrB2–SiC and TiB_2–SiC composites materials that leads to increase the cutting speed as seen in Figure 2.4. Maximum temperature reduces with SiC addition in all cases of diborides which causes an increase in cutting speed and efficiency.

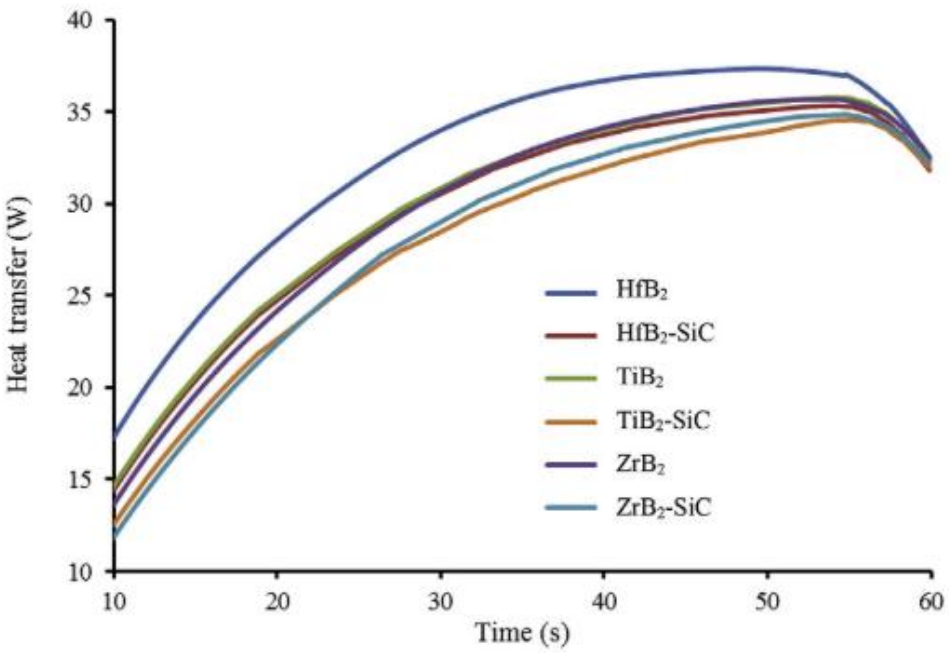

Figure 2.4: Heat dissipation from cutting tool by conduction to holder [35].

Zhang et al. [36] investigated a new drilling technology with ultra-high-speed diamond drilling which can accomplish high rates of penetration with lower energy and load. ABAQUS program was used to investigate the effect of ultra-high cutting speed on the cutting heat and rock breaking performance of a single cutter. It is indicated that the heat flux and specific energy drop with the increase of the rotary speed at cutting speed exceeds equals to 8 m/s. Fernandes et al. [37] studied thermal conductivity enhancement of a novel cemented carbide cutting tool during the design and building processing. In specified strategic areas, this concept integrates copper heat sinks, produced using advanced laser green lightweight machining. For WC-Co/Cu, a thermal conductivity of 127 W/m. K, considerably higher than that of WC-Co (36 W/m. K), was obtained.

This approach to obtaining WC-Co/Cu cutting instruments has been found to be successful in raising thermal conductivity locally, especially in the vicinity of the cutting field.

Xia and Gillespie [38] studied the thermal distribution of the workpiece tool chip device in a thermal equilibrium state and in a quasi-static fashion. For this quasi-static model, two particular problems were approached innovatively. Firstly, a pair of translationally periodic limits were used to model the shear plane in the shear field, which preserves temperature smoothness and velocity discontinuity without the need for extra-ordinary mesh refinement. Secondly, the heat flux was avoided by using straight chip boundaries because of the non-realistic material flow crossing the air-material boundaries. The relationship between the temperature and cutting speed was clarified in Figure 2.5 for the friction and shear field.

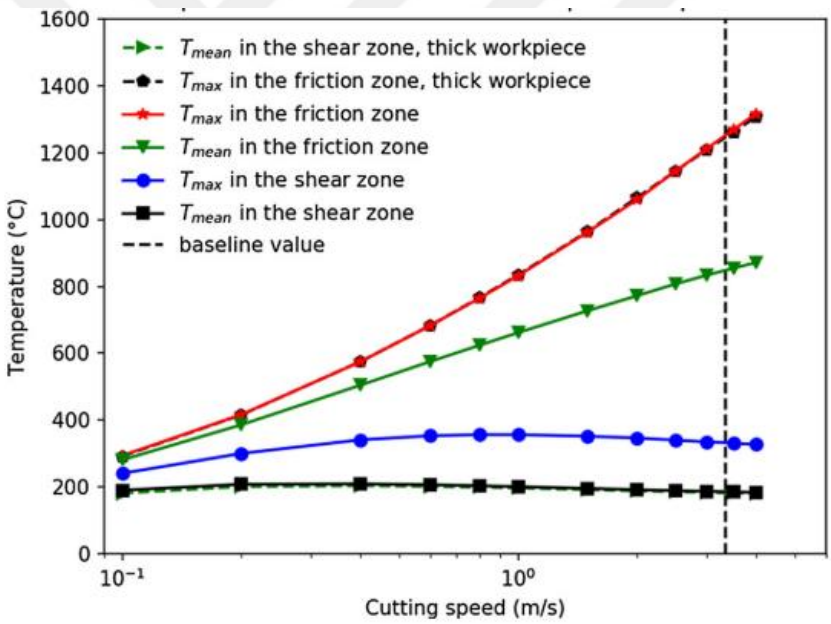

Figure 2.5: Impact of cutting speeds at the mean and maximum temperatures in the shear and friction zones [38].

2.3 CUTTING SPEED EFFECTS ON CUTTING TOOL LIFE

Motorcu [39] examined the wear of cutting tools such as the KY1615, KY4400, CBN / TiC cutting instruments for turning hardened steels under various conditions . In order to figure out the successful wear process, the worm surfaces of the cutting tools were analyses by the scanning electron microscope (SEM). In addition, the impacts on the tool life of cutting parameters and tool

hardness have been studied. With these cutting instruments, the surface roughness of hardened steels was also investigated. The lowest surface finish, which is about 0.884 µm, was provided by the CBN / TiC cutting instrument. The worst surface finish, however, was provided by the KY4400 cutting tool. Raja Durai et al. [40] studied the effect of the different forms of wear on the tool life of ceramic cutting tools based on alumina. For this reason, the use of alumina-based ceramic cutting tools while martensitic stainless steel was used to conduct comprehensive tool wear tests. The tool life of SiC whisker strengthened alumina ceramic cutting tools is influenced at a lower speed by flank wear, but at a higher speed by crater wear. In machining martensitic stainless steel, Ti [C, N] mixed alumina ceramic cutting tools have a significantly longer tool life than most alumina-based ceramic cutting tools.

Isik et al. [41] analyzed the effects of the temperature cutting velocity, the feed rate and the cutting depth. The heat distribution in the cutting tool, tool-chip interface, and workpiece provided valuable information regarding optimizing chosen cutting parameters. It was concluded that the cutting speed was the parameter that influenced the tool-chip interface temperature the most. The effect of the feed rate was not important. Both parameters have similar effects on the instrument's temperature. Significant improvements in the form and curvature of the chip were also noticed as the cutting speed increased. A 3-D finite element simulation model was also developed for the replication of the temperature based on the predicted heat over the tool-chip touch area, as seen in Figure 2.7. Broad agreement was discovered between the temperature values obtained by the finite component and the experimental findings, suggesting that the FEM heat distribution model was deliberately designed for future use.

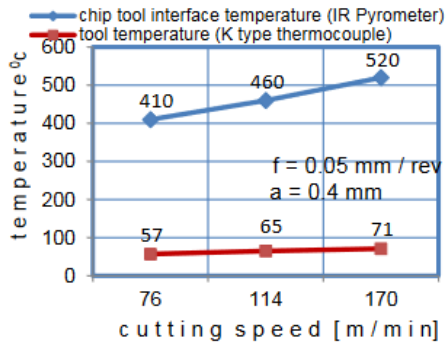

Figure 2.6: The influence of cutting speed and feed rate on temperatures [41].

Oganyan et al. [42] researched performance enhancement of end milling of titanium alloys Instead of instruments with multilayered composite nano-structured coatings Zr-ZrN-(Zr, Al)N and Zr-ZrN-(Zr,Cr, Al)N. The findings revealed that the brittle fracturing of the coating on the rake face and severe delamination's with large torn-off fragments of the coatings is common for the instruments with the Ti-TiN and Ti-TiN-(Ti, Al)N coatings, and this may suggest extreme adhesive-fatigue and inter-diffusion processes. The considerably more balanced wear process is common for the instruments with Zr-ZrN-(Zr, Al)N and Zr-ZrN-(Zr, Cr, Al)N coatings, the coating on the rake face usually maintains its integrity, and abrasive wear is more noticeable. It can be inferred that zirconium nitride based multilayered composite nanostructured coatings can be effectively applied as wear-resistant coatings in the final milling of titanium alloys.

Salonitis and Kolios [43] explored for the remaining life of the cutting instruments based on sophisticated approximation techniques, a novel reliability estimation methodology. For the representation of flank wear as a function of process parameters and cutting powers, an approximation model is used that is based on a reaction surface and a proxy model. The interaction of cutting forces with flank wear is experimentally explored for the creation of this model. The findings demonstrate that, based on a minimal number of experimental runs, the suggested approach is an optimal method for determining the efficiency of the cutting instrument. Experimental verification of the titanium milling case supports the results of the current report.

2.4 THE NOVELTY OF THE STUDY

From the above-mentioned previous literature review, it is indicated that many papers studied the temperature distribution in cutting tool experimentally with the aid of COMSOL software. Also, some researchers investigated the effect of heat flux and the maximum temperature on cutting tools for Al_2O_3 and steel. ANSYS software wasn't utilized for study temperature distribution. In addition, fewer papers studied the cutting of diboride materials.

Therefore, in this study, a numerical approach by ANSYS software for the first time will be utilized to study the temperature distribution and heat transfer parameters in cutting tool fabricated from Aluminum-Oxide, Zirconium Diboride, Titanium Diboride and Titanium Nitrite. The effect of changing the type of the material of the cutting tool will be investigated on four materials. The heat transfer characteristics and temperature distribution to determine the minimum, maximum,

and optimum values of the temperature of the cutting tool have been investigated. The effect of the cutting speed on the temperature of the cutting process will be investigated while the speed will be varied from 180 to 220 m/min and feed rate will be studied with three different values (0.138, 0.277, and 0.554 mm/rev). The study of cutting tool life with the different materials will be introduced. An optimization will be performed to determine the superlative cutting tool and the machining parameters.

3. NUMERICAL STUDY

3.1 MATERIAL SELECTION

In this research, the temperature and heat flux distribution in cutting tool processing four materials of Al_2O_3, ZrB_2, TiB_2 and TiN have been examined. Two diboride materials will be utilized as they have good properties such as wear-resistance and withstand against ultra-high temperatures as seen in Table 3.1. The workpiece and the holder are made from the AISI1045 steel with properties as stated in

Table 3.2.

Table 3.1: Specifications of the cutting tool materials.

Material	Chemical form	Density ρ (kg/m^3)	Thermal conductivity k (W/m. K)	Specific heat C_P (J/kg. K)
Aluminum oxide	Al_2O_3	3950	12	651
Zirconium diboride	ZrB_2	6080	18	587
Titanium diboride	TiB_2	4520	24	554
Titanium nitrite	TiN	5400	27	327

Table 3.2: properties of workpiece and holder materials.

AISI1045 steel properties	Magnitude	Unit
Density	7870	kg/m^3
Thermal conductivity	51.9	W/m. K
Tensile strength	585	MPa
Yield strength	450	MPa
Poisson's ratio	0.29	

3.2 GEOMETRY OF THE TOOL

Figure 3.1 shows the 3D model of a cutting tool consisting of insert, shim, and cutting holder, where the shim is positioned between the insert and the cutting holder. SOLIDWORKS software

was used to construct the three-dimensional model that was utilized in the tests. The specific dimensions of the insert and the holder are similar to the model utilized in [32] are illustrated in Figure 3.2 where the elevation and side views, as well as the plan view, show the thickness of the inserts with 4.7 mm and about 110 length of the steel holder.

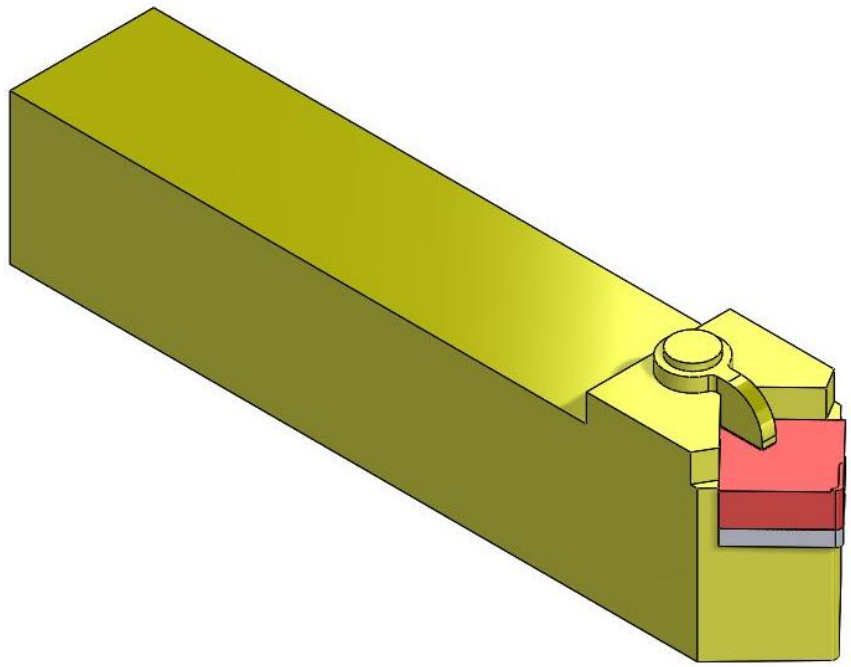

Figure 3.1: Three-dimensional model of the geometry of insert and cutting holder.

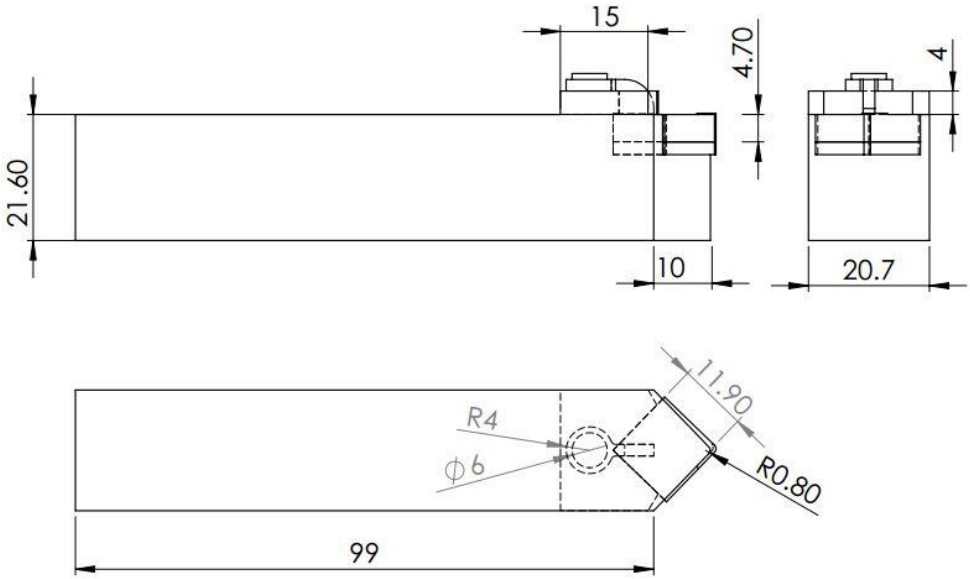

Figure 3.2: The dimensions of the cutting tool with insert and cutting holder.

Figure 3.3 shows the area of clamping between the insert and the cutting holder and the area of the flux between the insert and the workpiece. 12.7 x 12.7 mm insert with 4.7 mm in thickness was used to study the temperature distribution in the hall cutting tool with the average, minimum and maximum values and their positions.

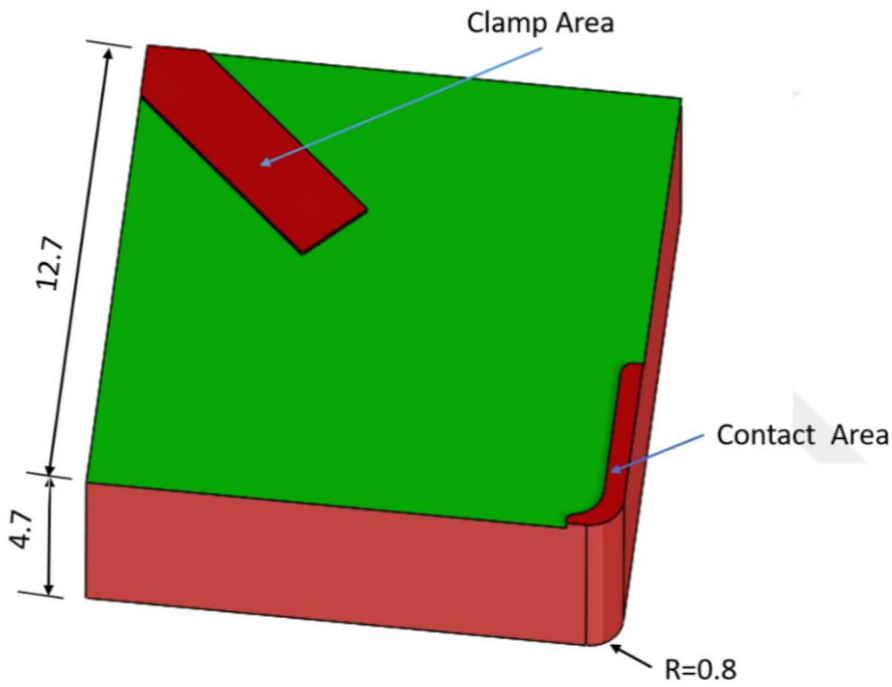

Figure 3.3: Dimensions of the insert and contact area between the inset and the workpiece.

3.3 NUMERICAL METHOD

3.3.1 Physical Model

The model was drawn by SOLIDWORKS software then the ANSYS fluent software was utilized to set up the boundary conditions and simulate the heat flux between the insert and the workpiece and temperature distribution.

3.3.2 Meshing

The unstructured meshing was chosen for the computational domain cause of the complexity of the model. The mesh generation in the regions of heat flux and clamp area have refinement to increase the quality of the grids. Simulation results can be seen in Figure 3.4 and Figure 3.5. To confirm the solution independency of the mesh, the grid-dependency is checked for four different grids: 456187, 625471, 820142, and 1242347cells, respectively. The specific details of the meshing of the insert were indicated in Figure 3.6. The error in average temperature and heat flux are tested in the cases of the four conditions and it is indicated the lowest error in all tests achieved with 1242347 elements as seen in Table 3.3 and no change in results with increasing number of elements after this condition so that this is used for this study.

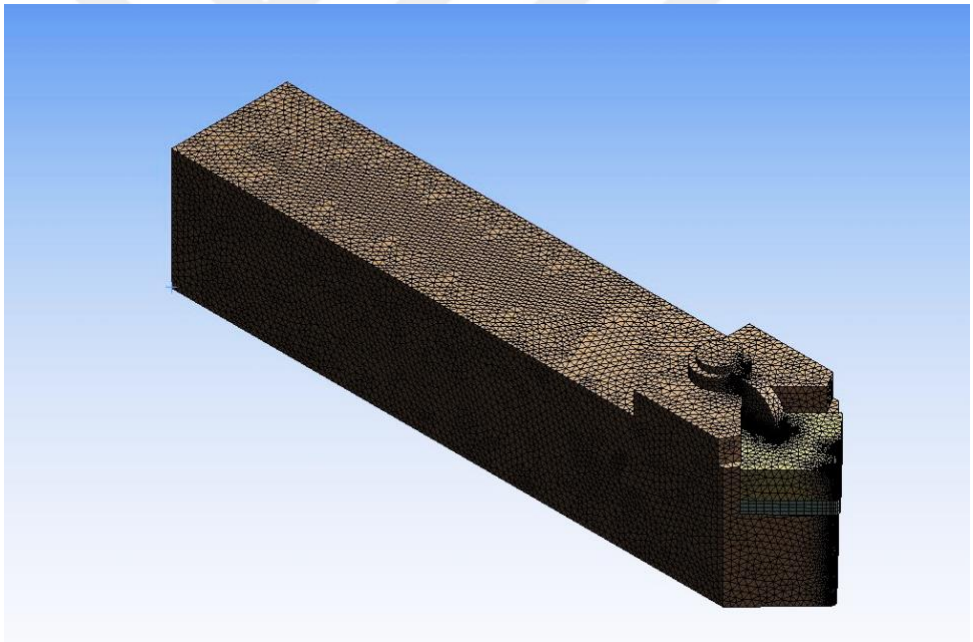

Figure 3.4: 3D of mesh generation grids.

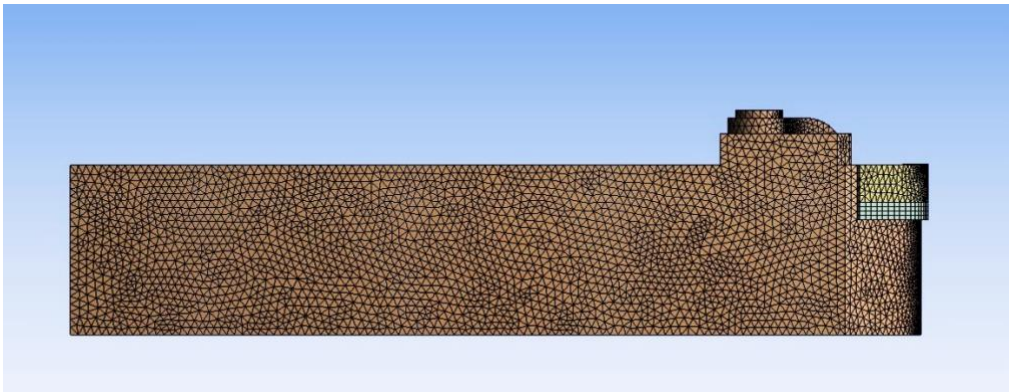

Figure 3.5: Elevation view of the grid generation.

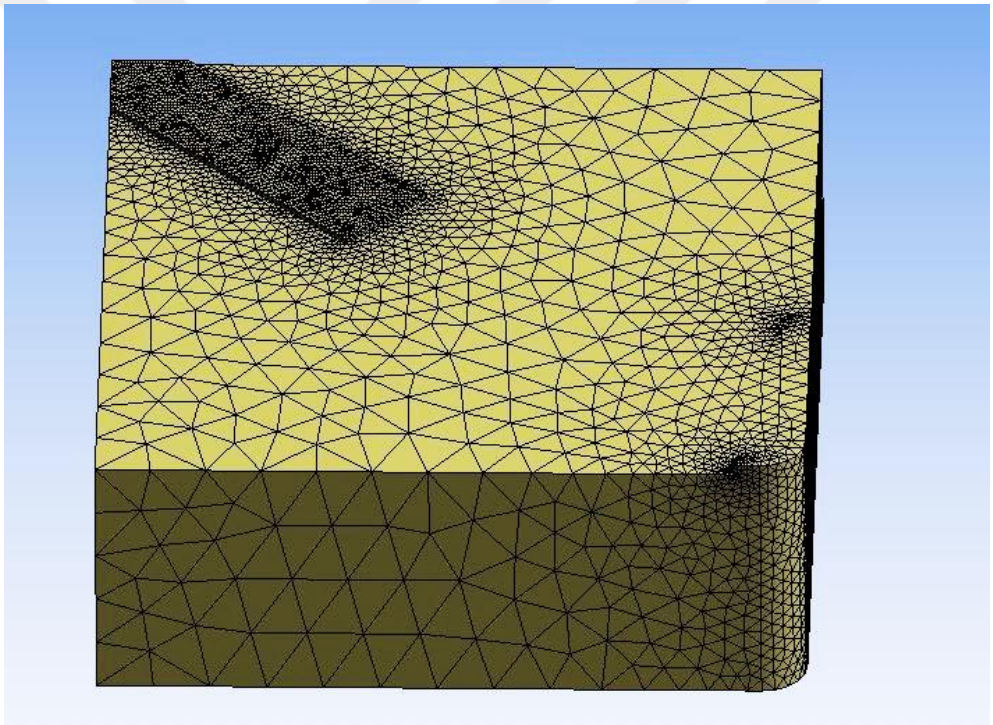

Figure 3.6: Mesh generation of the insert.

Table 3.3: Error percentage of average temperature and heat flux.

Meshing elements number	456187	625471	820142	1242347
Average Temperature Error	5.64%	3.0124%	1.921%	1.134
Heat flux Error	4.84%	2.451%	1.421%	0.927

3.3.3 Governing Equations

Heat conduction equation that describes the thermal model may be described by the nonlinear transient three-dimensional diffusion equation:

$$\rho C_p \frac{\partial T}{\partial t} = \vec{\nabla}(k \vec{\nabla} T) \quad (1)$$

Where t is the time in second and T is the temperature in kelvin unit while k expresses the thermal conductivity in W/m. K and C_p for the specific heat in J/kg. K and ρ determine the density of the material in kg/m^3. Heat convection and radiation can be calculated by the following relation:

$$-K \frac{\partial T}{\partial n} = h(T - T_\infty) + \sigma \varepsilon (T^4 - T_\infty{}^4) \quad (2)$$

Heat flux was applied for the contact between the insert and the workpiece can be determined by:

$$\dot{q} = C_p \frac{\partial T}{\partial t} \quad (3)$$

Where the equation of the heat flux that was used in the UDF code:

$$\dot{q} = 0.4926\, t^5 - 97.19\, t^4 + 6914\, t^3 - 232532 t^2 + 4000000 t + 10000000 \quad (4)$$

The cutting tool life can be calculated based on the cutting speed and parameter constants.

$$v\, t^n = C \quad (5)$$

Where v is the cutting speed, t is the tool life in minute's unit. n and C are parameters that depend on feed, depth of cut, work material, tooling material, and the tool life criterion used. n is the slope of the plot and C is the intercept on the speed axis at one-minute tool life. To calculate n and c parameters for Al_2O_3, those steps can be followed: At t =1 min, $v = C = 270$ m/min

At t=25 min the v =180 m/min and $v\, t^n = C$ so that

$180\ 25^n = 270$

$n = 0.126$, so that

$v\, t^{0.126} = 270$ (6)

The constants (C, n) for all materials are illustrated in Table 3.4.

Table 3.4: Constants parameters C and n for various materials.

Tool Material	C	n
Aluminum oxide	270	0.126
Zirconium diboride	285	0.117
Titanium diboride	293	0.124
Titanium nitrite	309	0.102

3.3.4 Boundary and Initial Condition

To simulate the heat transfer and temperature distribution for cutting, the heat flux equation at the contact area between the insert and the workpiece was generated by an excel program from the study [27] and [32]. UDF in ANSYS fluent was utilized to determine the boundary of the heat flux at the flux area according to the equation of flux. All the outer surface of the cutting tool was performed as a heat convection boundary equation where the surfaces between the insert and the holder was established as conduction heat transfer. The following assumptions are used in the numerical simulation:

- At the initial condition, the cutting insert, shim, and cutting holder have room temperature which is equal to 300 K.
- Heat flux was applied at the contact area interface according to the heat flux equation (4) at t = 0 s.
- The cutting process continues up to 60 seconds and then the heat load is removed.
- The heat transferred by conduction between the tool-shim and tool-holder interface.
- The cutting speed was changed from 180 to 220 m/min and the feed-rate has three different values such as 0.138, 0.277, and 0.554 mm/rev.

3.4 VALIDATION

For validation of the simulation results, the heat flux of the present study was compared with the previous studies [27] and [32] as seen in Figure 3.7. The temperature of the insert as an average value was compared with the same studies as shown in Figure 3.8. It is indicated that the deviation between the results is very limited. Therefore, the present numerical results have enough realistic accuracy. The regular differences between numerical and previous results for heat flux are around 2.34%. The highest dissimilarity for heat flux is 4.51% and the smallest dissimilarity is 1.03%. The validation results explained that the differences between the numerical and the experimental results are acceptable where the regular differences between numerical and previous results for average temperature is around 1.72%. The highest dissimilarity for average temperature is 2.87% and the smallest dissimilarity is 0.87%. In general, the differences are acceptable for simulation errors.

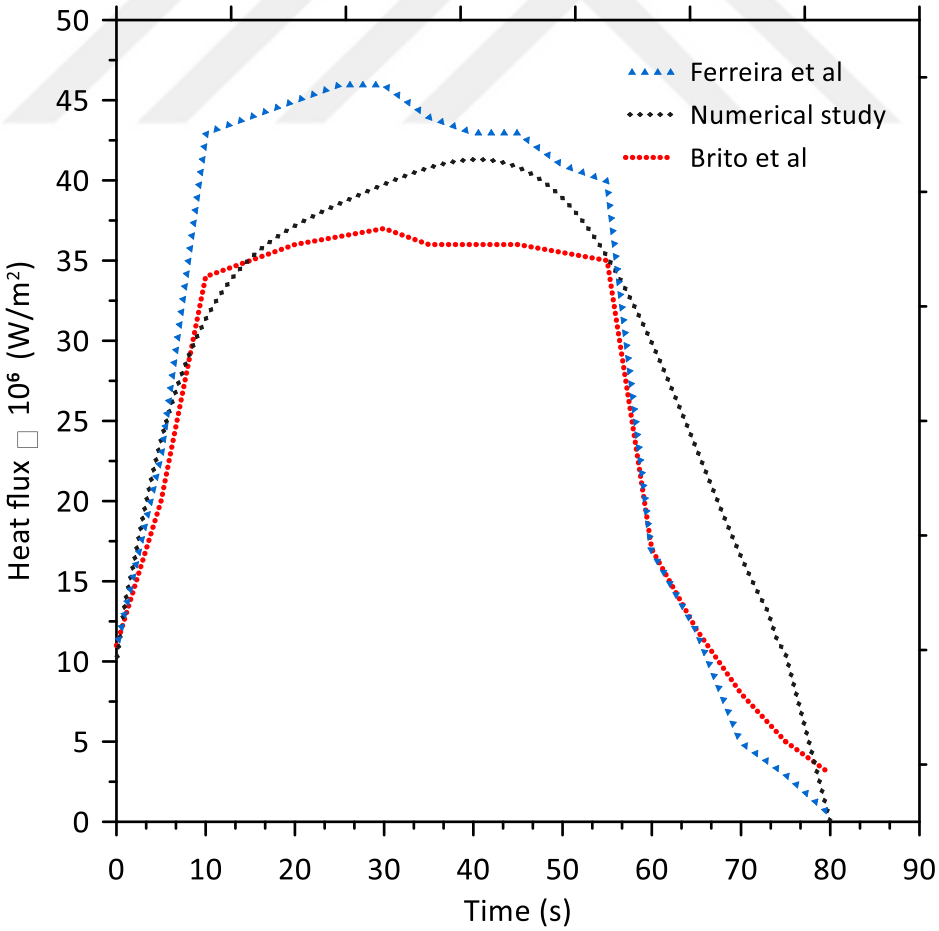

Figure 3.7: Comparison between the numerical results and the previous studies of Brito [27] and Ferreira [32] for the heat flux.

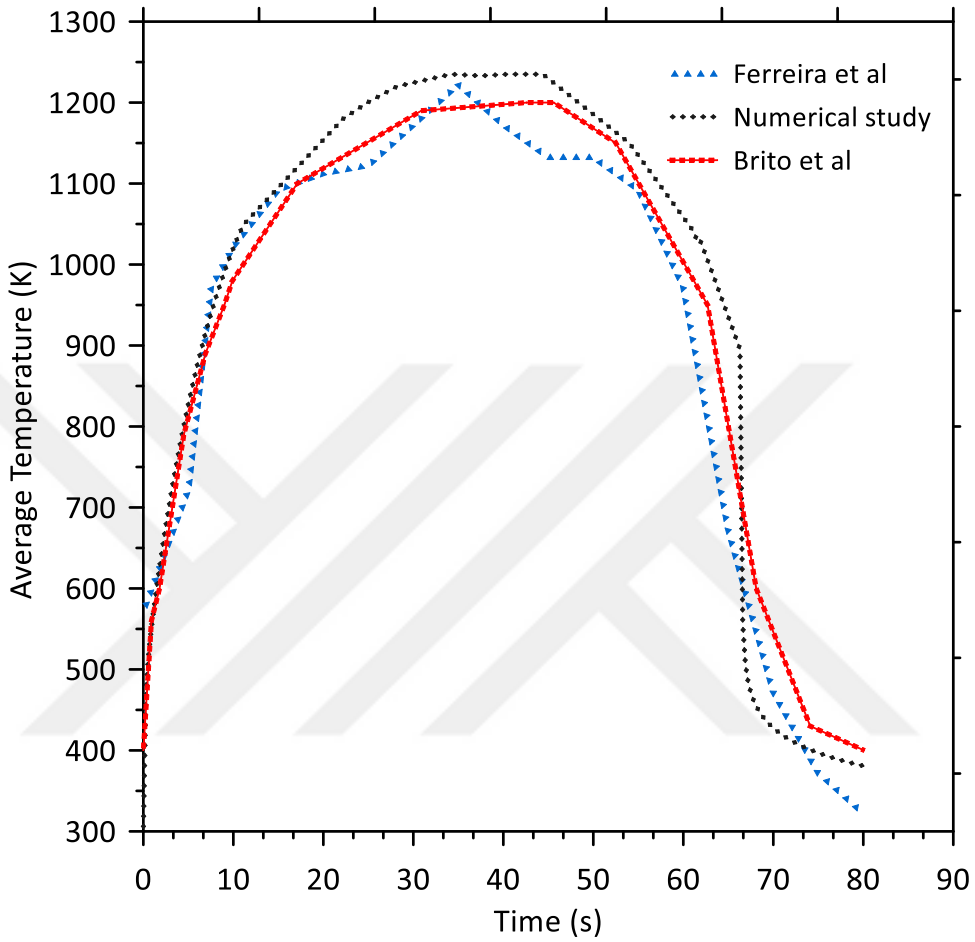

Figure 3.8: Comparison between the numerical results and the previous studies of Brito [27] and Ferreira [32] for the average temperature.

4. RESULTS AND DISCUSSIONS

In this section, the results to estimate the heat flux, temperature distribution maximum, and minimum temperature by using the inverse function of heat flux with software ANSYS FLUENT have been analyzed. At the beginning of the process, the cutting tool and holder were found at uniform room temperature. The cutting machining continues up to 60 seconds which is enough for reaching the steady-state and the maximum temperature can be determined. Heat flux is applied on the tool then the cutting is stopped and the tool moves off the workpiece.

4.1 TEMPERATURE VARIATION WITH TIME

Figure 4.1 shows the average temperature of the contact area during the cutting for Al_2O_3, ZrB_2, TiB_2, and TiN. It is indicated that the aluminum oxide achieved the highest temperature for the following figure about 1050 K comparing to other insert materials where the Titanium nitrite scored the lower values of temperature as near to 860 K.

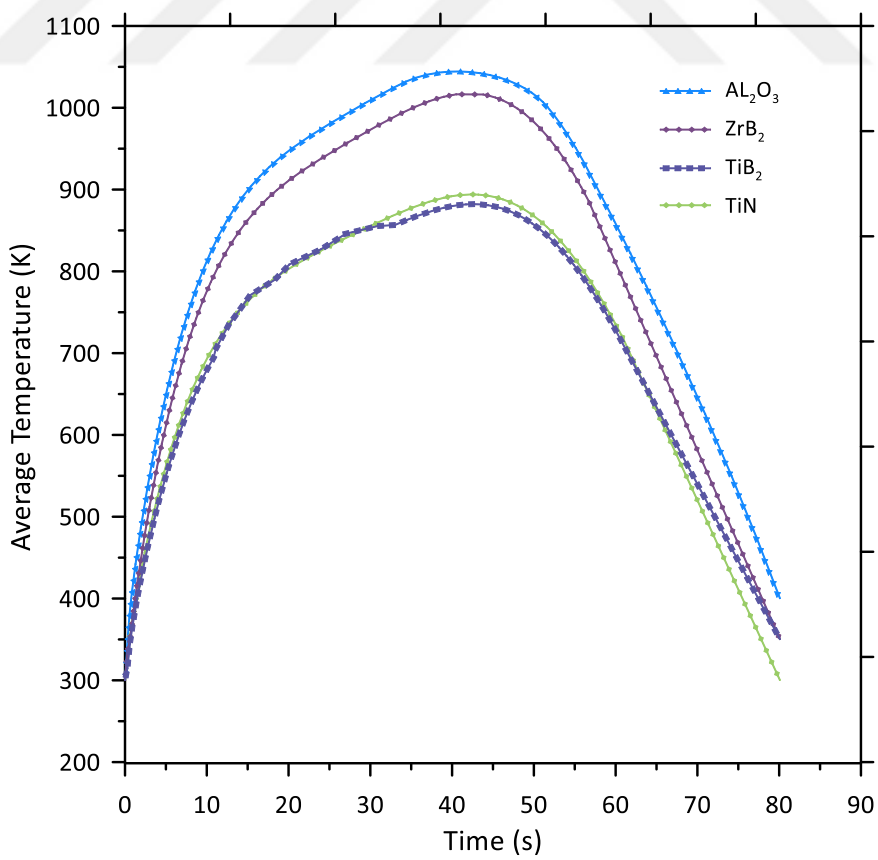

Figure 4.1: The average temperature of the contact area during the cutting for various materials.

The temperature begins to increase when the heat flux was applied until it reaches the maximum values near 50 seconds from the starting of the machining process. The temperature begins to decrease when the cutting tool goes away from the workpiece and there is no heat flux. It is indicated that the Zirconium diboride and Titanium diboride experienced lower average temperatures than aluminum oxide because of the low thermal conductivity of diboride materials. As it was mentioned, maximum temperature affects machining speed and the productivity rate. Figure 4.2 shows the maximum temperature of different materials aluminum-oxide, Zirconium diboride, Titanium diboride, and Titanium nitrite. It is indicated that the ZrB_2 and TiB_2 have improved performance and can work at higher speeds and increase the productivity. The minimum temperature for the face of the insert at heat flux was directed for the aluminum-oxide, Zirconium diboride, Titanium diboride and Titanium nitrite was illustrated in Figure 4.3. The maximum temperature for aluminum oxide is 1270 K where, the Titanium nitrite achieved 1090 K. At first, the applied heat flux heats the tip of the tool ,and then the thermal heat is dispersed in the cutting tool as time passes .The tool’s hot point is the chip interface at any given time .The contours reveal that most holder feels a change in temperature at low temperature. By conduction, the bulk of the produced heat is transmitted to the cutting holder and shim .This can also be inferred that the holder's higher mass has resulted in lower temperature increase within it .Radiation is essential, and the maximum heat losses are related to the radiation after conduction process.

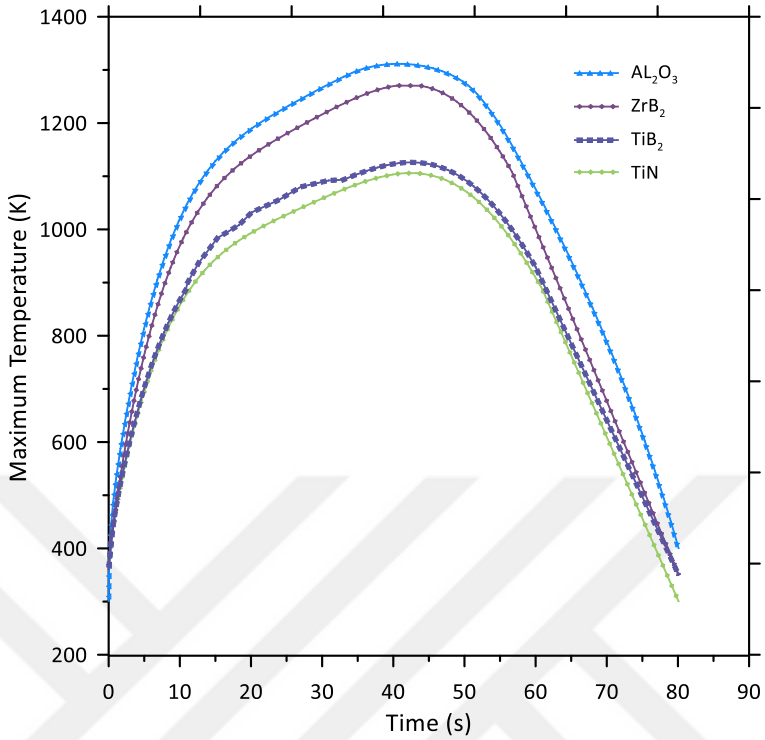

Figure 4.2: The maximum temperature of the contact area during the cutting for various materials.

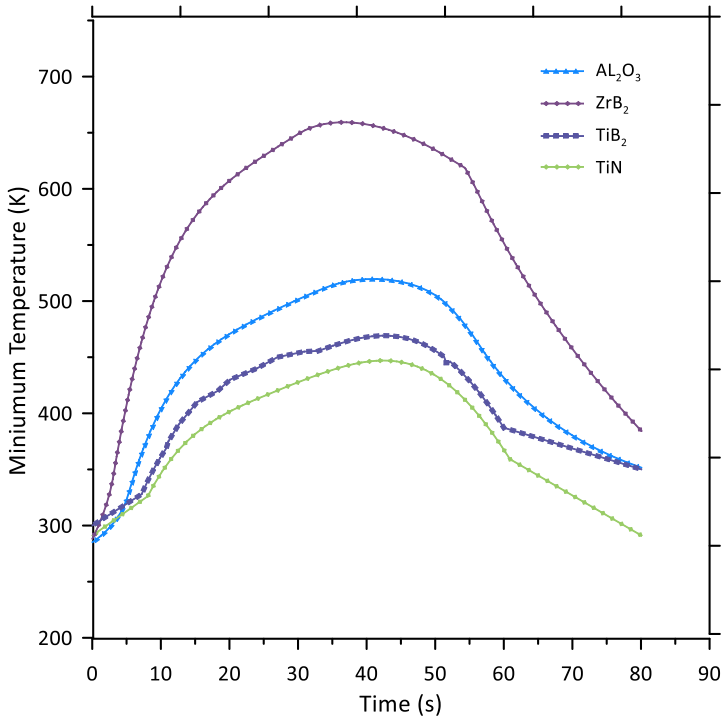

Figure 4.3: The minimum temperature of the contact area during the cutting for various materials.

4.2 INFLUENCE OF CUTTING CONDITIONS IN THE TEMPERATURE ESTIMATION

4.2.1 The Effect of Cutting Speed on the Temperature

Temperature changes obtained are directly proportional to the increase in cutting speed as seen in Figure 4.4. The temperature gradually increases with the rise of cutting speed for all the materials. The lowest temperature was obtained at a cutting speed of 180 m/min and the highest temperature was obtained at a cutting speed of 220 m/min. it can be observed that the TiN material is the better choice comparing to the other materials depending on the temperature distribution versus the cutting speed.

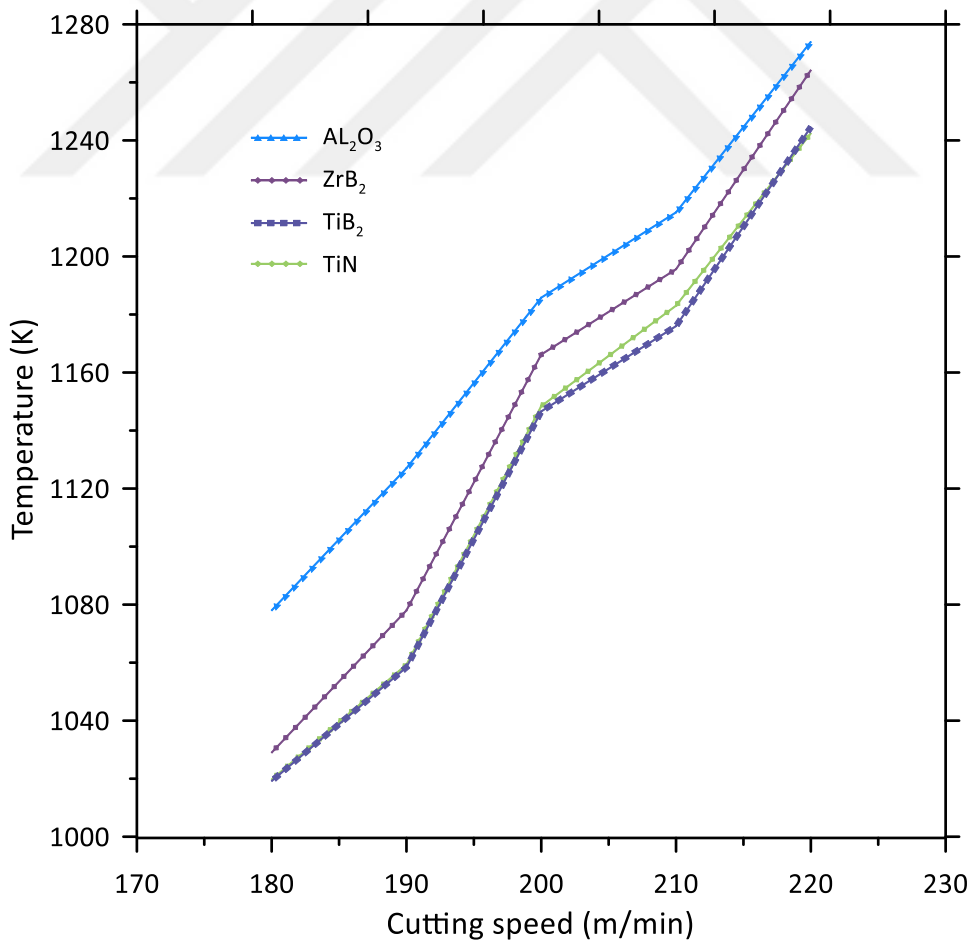

Figure 4.4: The relation between the temperature and the cutting speed of the cutting tool.

4.2.2 The Effect of Feed Rate on the Temperature

As the TiN achieved a better performance than the other materials, the feed-rate (FR) of the cutting tool with TiN was studied. The relation between the temperature and the FR of the cutting tool for TiN is illustrated in Figure 4.5. The higher the feed rate the higher the contact temperature of the interface. This behavior is due to higher feed rates, higher strain rates in primary and secondary shear zones.

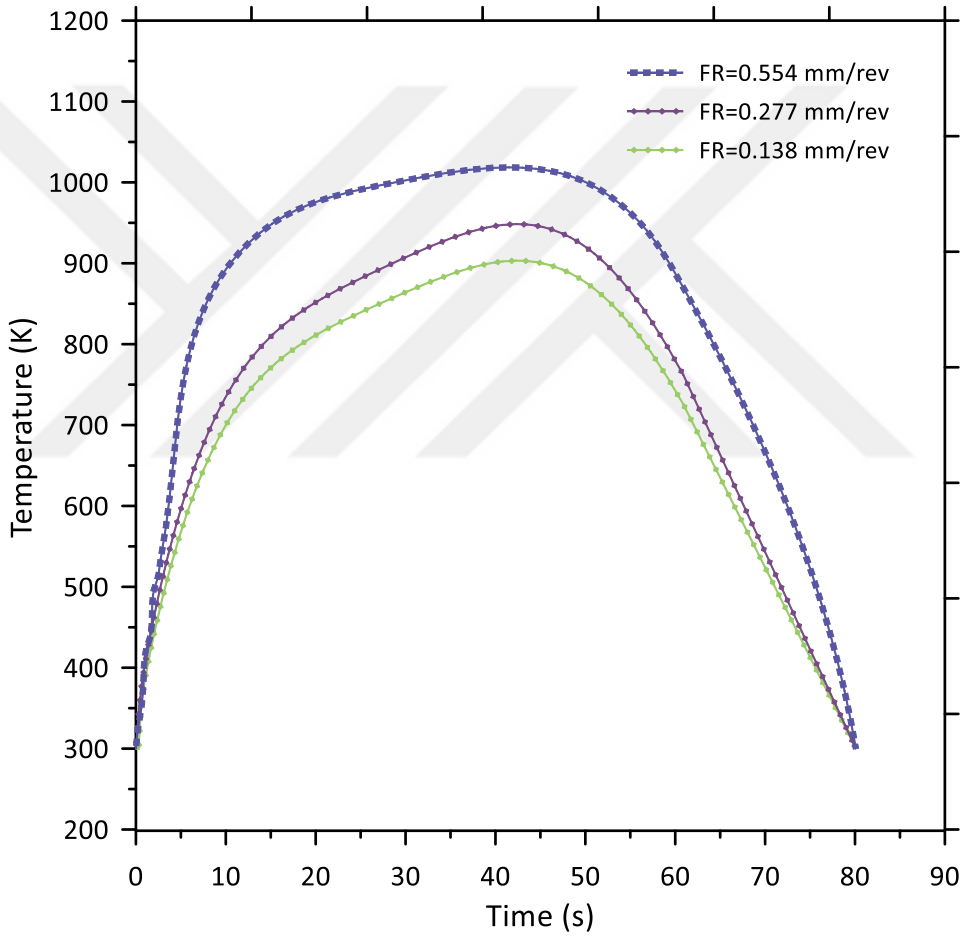

Figure 4.5: The relation between the temperature and the feed-rate FR of the cutting tool for TiN.

4.2.3 Influence of Cutting Speed on the Cutting Tool Life

The cutting tool life can be determined by many ways such as fracture failure when excessive cutting force leading to brittle fracture, temperature failure when cutting temperature is too high,

and gradual wear where the loss of tool shape and cutting efficiency resulting in gradual wearing of the cutting tool. In this study, the temperature failure will be used to determine the cutting tool life. Figure 4.6 shows the relation between the cutting tool life and cutting speed for various materials aluminum-oxide, Zirconium diboride, Titanium diboride, and Titanium nitrite. It can be seen that the cutting tool life decreased with the increase the cutting speed. The rise in cutting speed leads to an increase in removal materials where the temperature increases rapidly. The Titanium diboride achieved the maximum tool life comparing to cutting tools with the other materials. The maximum cutting tool life is indicated at 180 m/min with 59, 52, 45, and 32 min for aluminum-oxide, Titanium nitrite, Zirconium diboride, and Titanium diboride, respectively. High temperature was created by the increased cutting speed, which resulted in a rapid deterioration of the quality of the ceramic tool material and the cutting edge was then easily chipped by the cutting force.

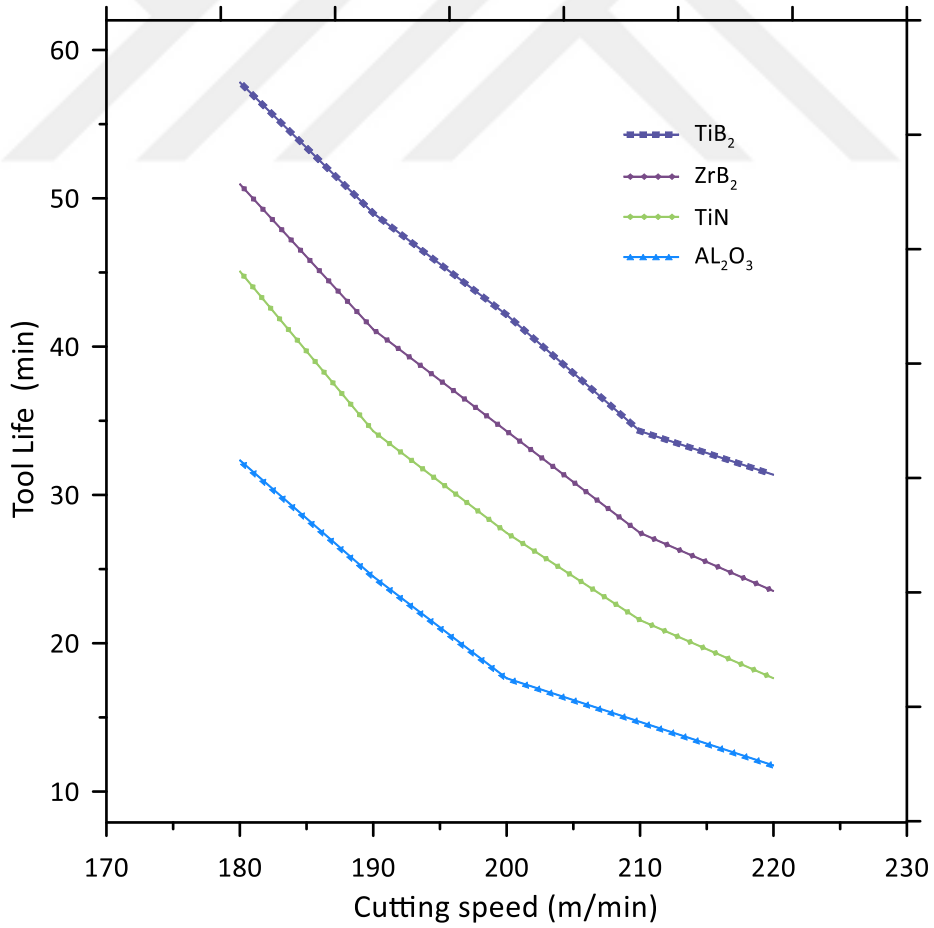

Figure 4.6: the relation between the cutting tool life and cutting speed for various materials.

4.3 TEMPERATURE DISTRIBUTION

The temperature distribution of insert, shim, and cutting holder at 5 s from the start of the cutting process is illustrated in Figure 4.7. It is indicated that the maximum temperate appeared at the contact area between the insert and the workpiece where the heat flux effect directly on the insert. It can be shown that most of the body of cutting holders have temperature equals to 300 K and this means that the heat does not reach all the regions of the holder.

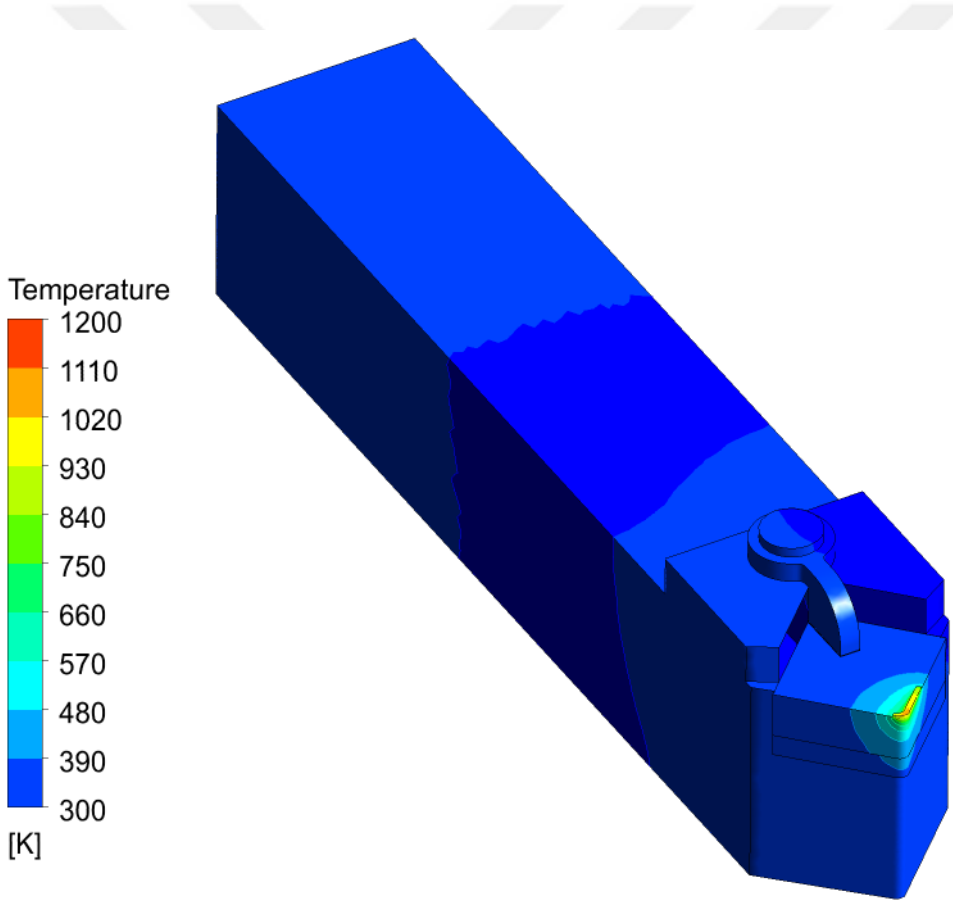

Figure 4.7: Contour of the temperature at 5 seconds.

Figure 4.8 shows the temperature distribution of the hall cutting tool at 20 s from the start of the machining operation. The temperature distribution of the cutting tool at 30 s, 40 s, and 50 s is illustrated in Figure 4.9, Figure 4.10, and Figure 4.11, respectively. It is indicated that the temperature increases with time for the insert and the heat transfer by conduction through the insert and then to the cutting holder. The heat transferred by convection from the outer surfaces to the surrounding leads to reduce the temperature of the body of the holder. The heat transferred by convection from the outer surfaces to the surrounding leads to reduce the temperature of the body of the holder. In the start, the tooltip was warmed by the applied heat flux, and then with the time spending, the thermal energy is dispersed in the tool. The tool's hot points are the devices controller at any moment .The simulation contours indicate that maximum holder practices a change in low temperature. The temperature profile increases more rapidly, and the average temperature values are reached prior than the reference case for a uniform heat distribution .The maximum interface temperature is found to rely heavily on the average heating intensity based on the estimation of two changed heating distributions .The first one of a stretched friction region leads to a lower average interface temperature ,although for the second heating distribution the significantly lower peak temperature is in an upstream position.

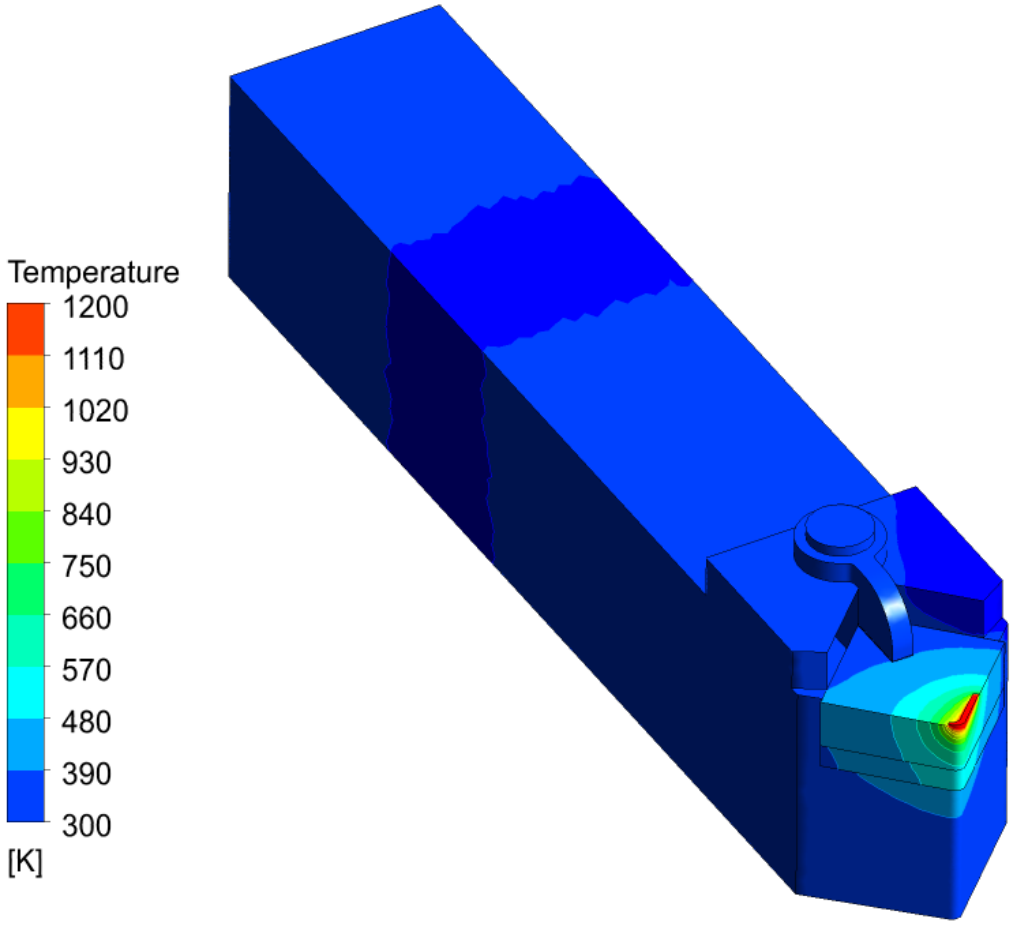

Figure 4.8: Contour of the temperature at 20 seconds.

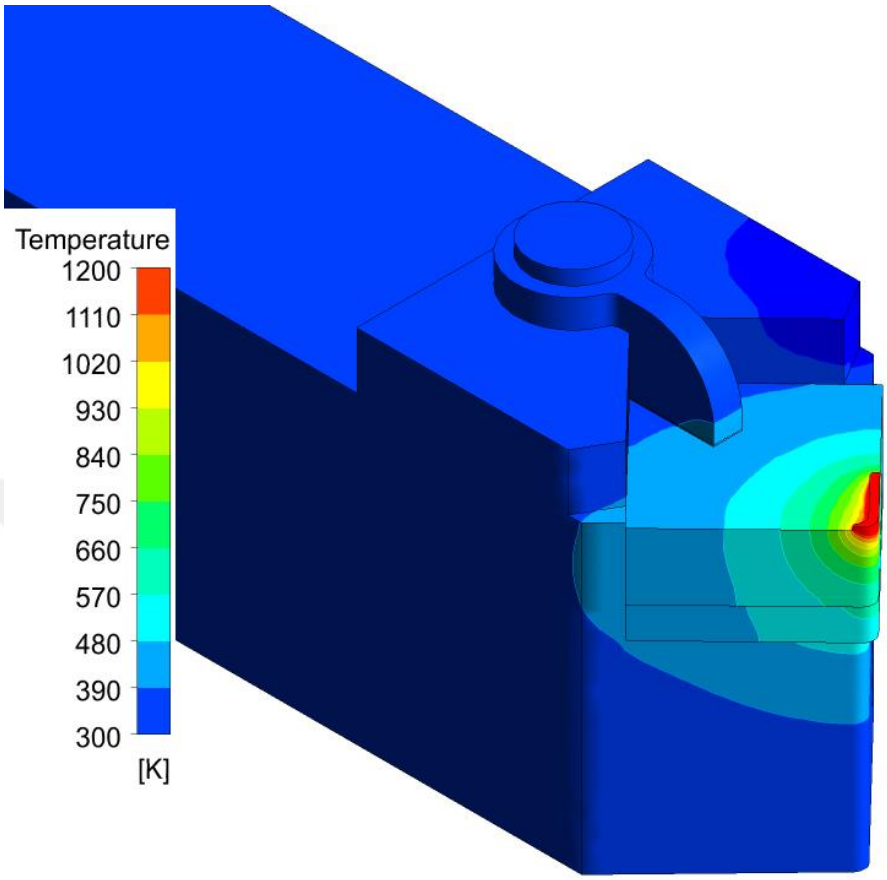

Figure 4.9: Contour of the temperature at 30 seconds.

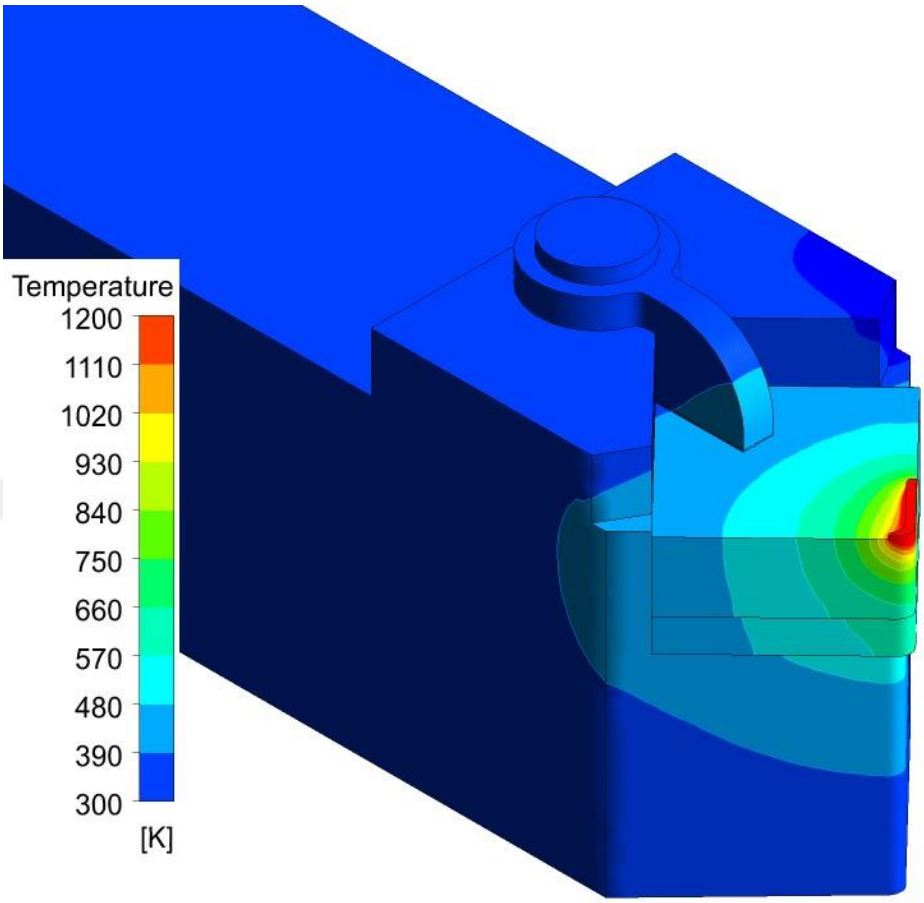

Figure 4.10: Contour of the temperature at 40 seconds.

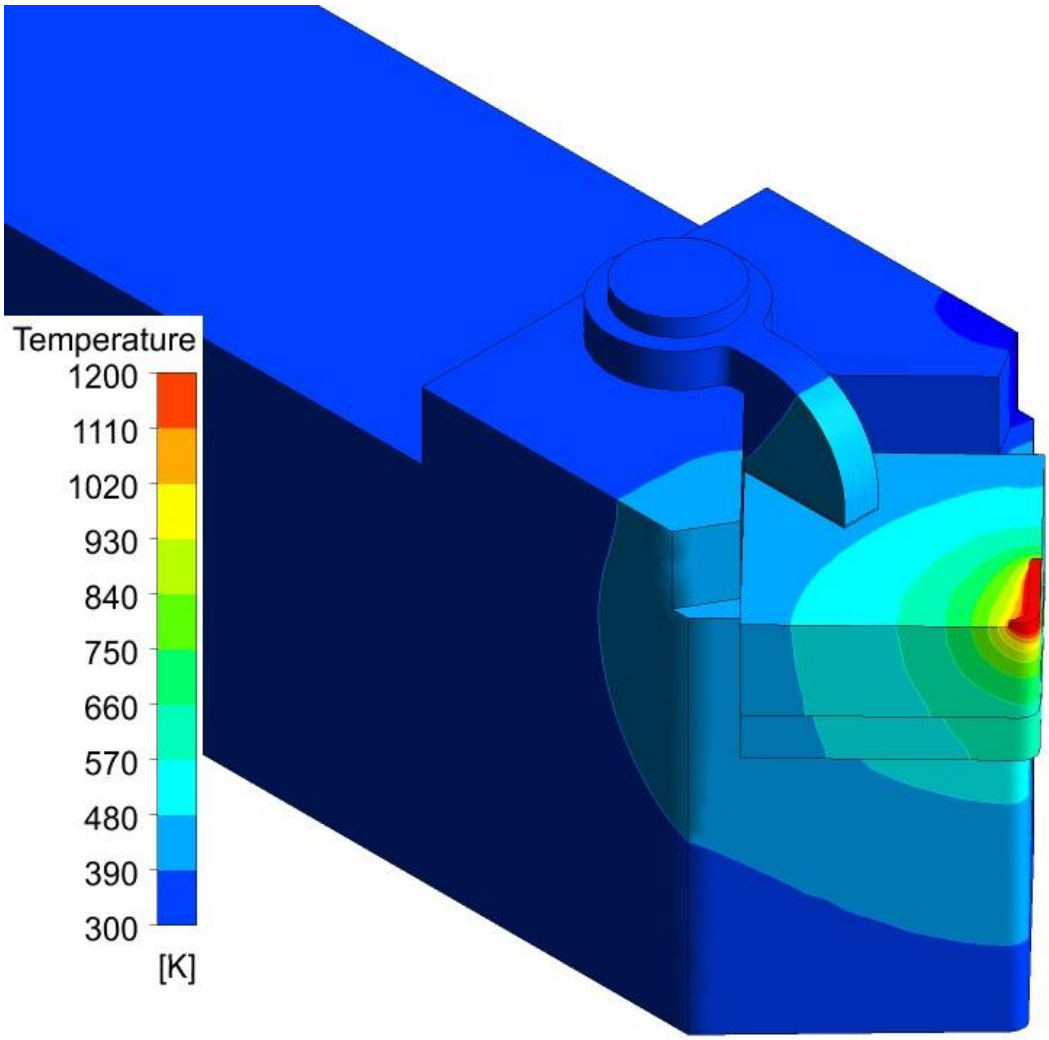

Figure 4.11: Contour of the temperature at 50 seconds.

5. CONCLUSION

In this study, the temperature distribution of insert, shim, and cutting holder for various materials have been investigated depending on the heat flux of the contact surface of heat generation. The UDF and ANSYS FLUENT were joined to specify the heat flux and temperature distribution. The various materials are utilized in this study such as Al_2O_3, ZrB_2, TiB_2, and TiN to indicate the effect of diboride materials improvement in cutting machining. The machining parameters such as the cutting speed varied from 180 to 220 m/min and feed rate with three different values such as 0.138, 0.277, and 0.554 mm/rev were investigated. The study of cutting tool life with the different materials was introduced. The results can be concluded in some points:

- It is indicated that the aluminum oxide achieved the highest average temperature following the number about 1050 K comparing to other insert materials where the Titanium nitrite scored the lower values of temperature with the number near to 860K.
- It is observed that the minimum temperatures were attained at a cut speed of 180 m/min and the maximum temperatures were achieved at a cutting speed of 220 m/min.
- The increase in cutting speed contributes to a rise in removal materials where the temperature is growing exponentially. Comparing to cutting tools with other materials,
- The TiN material achieved good behavior with cutting speeds of 180 m/min and 0.138 mm/rev.
- The Titanium diboride obtained the highest tool life so that the optimization process indicated that the TiB_2 is the respectable choice with machining parameters (cutting speed =180 m/min, and feed rate = 0.138 mm/rev) where the temperature distribution is acceptable.

6. FUTURE STUDY

The study of the temperature and heat flux distribution for the cutting material and workpiece from mixing powders may be advised for the future studies.

REFERENCES

[1] C. Rao, R. Kiran, and P. J. M. Asha, "Influence of machining parameters on cutting tool life while machining aluminum alloy fly ash composite," vol. 149, p. 012157, 2016.

[2] M. P. Kumar, K. Amarnath, M. S. J. I. J. o. E. Kumar, and M. Research, "A review on heat generation in metal cutting," vol. 5, pp. 193-197, 2015.

[3] C. Ming, S. Fanghong, W. Haili, Y. Renwei, Q. Zhenghong, and Z. Shuqiao, "Experimental research on the dynamic characteristics of the cutting temperature in the process of high-speed milling," Journal of Materials Processing Technology, vol. 138, pp. 468-471, 2003/07/20/ 2003. Available: http://www.sciencedirect.com/science/article/pii/S0924013603001201

[4] S. Lo Casto, E. Lo Valvo, M. Piacentini, V. F. Ruisi, E. Lucchini, S. Maschio, et al., "Cutting Temperatures Evaluation in Ceramic Tools: Experimental Tests, Numerical Analysis and SEM Observations," CIRP Annals, vol. 43, pp. 73-76, 1994.

[5] H. Ay and W.-J. Yang, "Heat transfer and life of metal cutting tools in turning," International Journal of Heat and Mass Transfer, vol. 41, pp. 613-623, 1998/02/01/ 1998. Available: http://www.sciencedirect.com/science/article/pii/S0017931097001051

[6] V. Ostafiev, A. Kharkevich, K. Weinert, and S. Ostafiev, "Tool heat transfer in orthogonal metal cutting," 1999.

[7] J. C. Rozzi, F. E. Pfefferkorn, F. P. Incropera, Y. C. J. I. j. o. h. Shin, and m. transfer, "Transient, three-dimensional heat transfer model for the laser assisted machining of silicon nitride: I. Comparison of predictions with measured surface temperature histories," vol. 43, pp. 1409-1424, 2000.

[8] W. Grzesik and C. A. van Luttervelt, "An Investigation of the Thermal Effects in Orthogonal Cutting Associated with Multilayer Coatings," CIRP Annals, vol. 50, pp. 53-56, 2001/01/01/ 2001. Available: http://www.sciencedirect.com/science/article/pii/S0007850607620691

[9] I. Lazoglu and Y. Altintas, "Prediction of tool and chip temperature in continuous and interrupted machining," International Journal of Machine Tools and Manufacture, vol. 42, pp. 1011-1022, 2002/07/01/ 2002. Available: http://www.sciencedirect.com/science/article/pii/S0890695502000391

[10] T. Harris, E. Brookes, C. J. I. J. o. R. M. Taylor, and H. Materials, "The effect of temperature on the hardness of polycrystalline cubic boron nitride cutting tool materials," vol. 22, pp. 105-110, 2004.

[11] V. Dessoly, S. N. Melkote, and C. Lescalier, "Modeling and verification of cutting tool temperatures in rotary tool turning of hardened steel," International Journal of Machine Tools and Manufacture, vol. 44, pp. 1463-1470, 2004/11/01/ 2004. Available: http://www.sciencedirect.com/science/article/pii/S0890695504001294

[12] J. Rech, J. L. Battaglia, and A. Moisan, "Thermal influence of cutting tool coatings," Journal of Materials Processing Technology, vol. 159, pp. 119-124, 2005/01/10/ 2005. Available: http://www.sciencedirect.com/science/article/pii/S0924013604007885

[13] W. Grzesik, "Determination of temperature distribution in the cutting zone using hybrid analytical-FEM technique," International Journal of Machine Tools and Manufacture, vol. 46, pp. 651-658, 2006/05/01/ 2006. Available: http://www.sciencedirect.com/science/article/pii/S0890695505001641

[14] E. Ceretti, L. Filice, D. Umbrello, and F. J. C. a. Micari, "ALE simulation of orthogonal cutting: a new approach to model heat transfer phenomena at the tool-chip interface," vol. 56, pp. 69-72, 2007.

[15] B. Yilbas, A. Arif, C. Karatas, and M. J. A. S. S. Ahsan, "Cemented carbide cutting tool: Laser processing and thermal stress analysis," vol. 253, pp. 5544-5552, 2007.

[16] R. Kountanya, "Cutting tool temperatures in interrupted cutting—The effect of feed-direction modulation," Journal of Manufacturing Processes, vol. 10, pp. 47-55, 2008/07/01/ 2008. Available: http://www.sciencedirect.com/science/article/pii/S1526612509000218

[17] R. F. Brito, S. R. d. Carvalho, S. M. M. d. Lima e Silva, and J. R. Ferreira, "Thermal analysis in coated cutting tools," International Communications in Heat and Mass Transfer, vol. 36, pp. 314-321, 2009/04/01/ 2009. Available: http://www.sciencedirect.com/science/article/pii/S0735193309000165

[18] K. Kadirgama, M. Noor, M. Rahman, W. Harun, and C. J. E. j. o. s. r. Haron, "Finite element analysis and statistical method to determine temperature distribution on cutting tool in end-milling," vol. 30, pp. 451-463, 2009.

[19] K. Kadirgama, M. Noor, K. Abou-El-Hossein, H. Habeeb, M. Rahman, B. Mohamad, et al., "Effect of dry cutting on force and tool life when machining aerospace material," vol. 4, 2010.

[20] J. C. Rozzi, W. Chen, and E. E. Archibald, "Indirect cooling of a cutting tool," ed: Google Patents, 2011.

[21] O. Verezub, Z. Kálazi, A. Sytcheva, L. Kuzsella, G. Buza, N. Verezub, et al., "Performance of a cutting tool made of steel matrix surface nano-composite produced by in situ laser melt injection technology," vol. 211, pp. 750-758, 2011.

[22] J. Martan and P. Beneš, "Thermal properties of cutting tool coatings at high temperatures," Thermochimica Acta, vol. 539, pp. 51-55, 2012/07/10/ 2012. Available: http://www.sciencedirect.com/science/article/pii/S0040603112001554

[23] B. Haddag and M. Nouari, "Tool wear and heat transfer analyses in dry machining based on multi-steps numerical modelling and experimental validation," Wear, vol. 302, pp. 1158-1170, 2013/04/01/ 2013. Available: http://www.sciencedirect.com/science/article/pii/S0043164813000483

[24] T. Yashiro, T. Ogawa, H. J. I. J. o. M. T. Sasahara, and Manufacture, "Temperature measurement of cutting tool and machined surface layer in milling of CFRP," vol. 70, pp. 63-69, 2013.

[25] S. Shu, K. Cheng, H. Ding, and S. Chen, "An Innovative Method to Measure the Cutting Temperature in Process by Using an Internally Cooled Smart Cutting Tool," Journal of Manufacturing Science and Engineering, vol. 135, 2013.

[26] S. Pervaiz, I. Deiab, E. M. Wahba, A. Rashid, and M. Nicolescu, "A Coupled FE and CFD Approach to Predict the Cutting Tool Temperature Profile in Machining," Procedia CIRP, vol. 17, pp. 750-754, 2014.

[27] R. F. Brito, S. R. Carvalho, and S. M. M. Lima E Silva, "Experimental investigation of thermal aspects in a cutting tool using comsol and inverse problem," Applied Thermal Engineering, vol. 86, pp. 60-68, 2015/07/05/ 2015. Available: http://www.sciencedirect.com/science/article/pii/S1359431115003907

[28] G.-S. Su, Y.-K. Guo, X.-L. Song, and H. Tao, "Effects of high-pressure cutting fluid with different jetting paths on tool wear in cutting compacted graphite iron," Tribology International, vol. 103, pp. 289-297, 2016/11/01/ 2016. Available: http://www.sciencedirect.com/science/article/pii/S0301679X16302006

[29] W. Baohai, C. Di, H. Xiaodong, Z. Dinghua, and T. J. C. J. o. A. Kai, "Cutting tool temperature prediction method using analytical model for end milling," vol. 29, pp. 1788-1794, 2016.

[30] A. Saini, B. Pabla, and S. J. P. o. t. I. o. M. E. Dhami, Part B: Journal of Engineering Manufacture, "Developments in cutting tool technology in improving machinability of Ti6Al4V alloy: a review," vol. 230, pp. 1977-1989, 2016.

[31] Y. Zhang, Y. Yang, Q. Li, and Y. Li, "Study on heat transfer model of coolant boundary layer during high speed cutting process," International Journal of Heat and Mass Transfer, vol. 114, pp. 1304-1313, 2017.

[32] D. C. Ferreira, E. d. S. Magalhães, R. F. Brito, and S. M. M. Lima E Silva, "Numerical analysis of the influence of coatings on a cutting tool using COMSOL," The International Journal of Advanced Manufacturing Technology, vol. 97, pp. 1305-1314, 2018/07/01 2018. Available: https://doi.org/10.1007/s00170-018-1855-7

[33] S. Berezvai, T. G. Molnar, A. Kossa, D. Bachrathy, and G. Stepan, "Numerical and experimental investigation of contact length during orthogonal cutting," Materials Today: Proceedings, vol. 12, pp. 329-334, 2019.

[34] A. K. Parida and K. Maity, "Numerical and experimental analysis of specific cutting energy in hot turning of Inconel 718," Measurement, vol. 133, pp. 361-369, 2019.

[35] F. Sadegh Moghanlou, M. Vajdi, J. Sha, A. Motallebzadeh, M. Shokouhimehr, and M. Shahedi Asl, "A numerical approach to the heat transfer in monolithic and SiC reinforced HfB2, ZrB2 and TiB2 ceramic cutting tools," Ceramics International, vol. 45, pp. 15892-15897, 2019.

[36] M. Gao, K. Zhang, Q. Zhou, H. Zhou, B. Liu, and G. Zheng, "Numerical investigations on the effect of ultra-high cutting speed on the cutting heat and rock-breaking performance of a single cutter," Journal of Petroleum Science and Engineering, vol. 190, 2020.

[37] B. Guimarães, C. M. Fernandes, D. Figueiredo, M. F. Cerqueira, O. Carvalho, F. S. Silva, et al., "A novel approach to reduce in-service temperature in WC-Co cutting tools," Ceramics International, vol. 46, pp. 3002-3008, 2020/02/15/ 2020. Available: http://www.sciencedirect.com/science/article/pii/S0272884219328354

[38] Q. Xia and D. R. H. Gillespie, "Quasi-static finite element modelling of thermal distribution and heat partitioning for the multi-component system of high speed metal cutting," Journal of Materials Processing Technology, vol. 275, 2020.

[39] A. R. Motorcu, "Tool life performances, wear mechanisms and surface roughness characteristics when turning austenised and quenched AISI 52100 bearing steel with ceramics and CBN/TiC cutting tools," 2011.

[40] A. Senthil Kumar, A. Raja Durai, and T. Sornakumar, "The effect of tool wear on tool life of alumina-based ceramic cutting tools while machining hardened martensitic stainless steel," Journal of Materials Processing Technology, vol. 173, pp. 151-156, 2006.

[41] A. Kus, Y. Isik, M. C. Cakir, S. Coşkun, and K. Özdemir, "Thermocouple and Infrared Sensor-Based Measurement of Temperature Distribution in Metal Cutting," Sensors (Basel, Switzerland), vol. 15, pp. 1274-91, 01/01 2014.

[42] A. Vereschaka, M. Oganyan, Y. Bublikov, N. Sitnikov, K. Deev, V. Pupchin, et al., "Increase in Efficiency of End Milling of Titanium Alloys Due to Tools with Multilayered Composite Nano-Structured Zr-ZrN-(Zr,Al)N and Zr-ZrN-(Zr,Cr,Al)N Coatings," Coatings, vol. 8, 2018.

[43] K. Salonitis and A. J. T. I. J. o. A. M. T. Kolios, "Force-based reliability estimation of remaining cutting tool life in titanium milling," vol. 106, pp. 3321-3333, 2020.